

## **Certificate in Clinician Performed Ultrasound (CCPU) Style Guide**

### **Neonatal Cranial Ultrasound**

**Disclaimer and Copyright:** Content within this curriculum was accurate at the time of publication. This curriculum is subject to Australian copyright law. Apart from any use as permitted by law, no part of this curriculum may be copied, adapted, reproduced or distributed without written permission from The Australasian Society for Ultrasound in Medicine (ASUM). All enquires to be directed to [education@asum.com.au](mailto:education@asum.com.au).

## Contents

### A systematic approach to the documentation of cranial ultrasound findings . 4

Key anatomical structures of the brain parenchyma .....	4
Evaluation of the ventricular system.....	5
Reporting of Germinal matrix/ intraventricular/periventricular haemorrhage (GMH/IVH) and periventricular leukomalacia (PVL).....	5
Evaluation of cerebrovascular system.....	6
Evaluation of superficial convexity of the brain .....	6
<b>Extra-axial space.....</b>	<b>6</b>
<b>Grey-white matter differentiation:.....</b>	<b>6</b>
Artefacts and anatomical variants.....	7

### Tables ..... 9

Table 1: Standard view via anterior fontanel - Coronal sections .....	9
Table 2: Standard view via anterior fontanel - Sagittal sections.....	10
Table 3: Supplemental views16-19 .....	11
Table 4: The ultrasound grading system for PVL has been described as follows <sup>21</sup> .....	13
Table 5: Differentiating physiological periventricular blush from PVL.....	14
Table 6: Papile's classification of GMH/IVH .....	15
Table 7: Proposed modification from Harris et al. <sup>3</sup> describing GMH/IVH.....	16

### Figures ..... 17

Figure 1: Coronal section showing hyperechoic basal ganglia suggestive of ischaemia and effaced ventricles suggestive of cerebral oedema.....	17
Figure 2: Parasagittal section showing hyperechoic parieto-occipital region suggestive of haemorrhage .....	17
Figure 3: Coronal section showing hyperechoic spots (periventricular calcification).....	18
Figure 4: Coronal section at Foramen of Monro showing the widest distance of the anterior horn of the lateral ventricle between the medial wall and the floor .....	18
Figure 5: Parasagittal view demonstrating maximum distance between the outermost point of the thalamus at its junction with the choroid plexus, and the outermost part of the occipital horn .....	19
Figure 6: Coronal section at Foramen of Monro showing the widest distance between the frontal horns (lateral to the lateral wall) at the level of the interventricular foramina of Monro .....	19
Figure 7: Coronal section showing a large intraventricular haemorrhage with midline shift.....	20
Figure 8: Midline sagittal section demonstrating anterior cerebral artery Doppler .....	20
Figure 9: Temporal view demonstrating middle cerebral artery Doppler .....	21

Figure 10: Sagittal and coronal section using high frequency transducer to demonstrate superior sagittal sinus flow .....	22
Figure 11: Sagittal and coronal section using high frequency transducer to demonstrate superior sagittal sinus thrombosis.....	23
Figure 12: Parasagittal section demonstrating lenticulostriate vasculopathy in 2D and colour Doppler	24
Figure 13: Coronal section using high frequency transducer.....	24
Figure 14: Coronal and sagittal sections showing hyperechoic periventricular halos showing radial striations.....	25
Figure 15: Diffuse, subtle, echogenic haze of the deep nuclei can be a normal finding in extremely preterm infants.....	26
Figure 16: Parasagittal view showing choroid plexus cyst .....	26
Figure 17: Parasagittal view showing connatal cysts .....	27
Figure 18: Section 1 (anterior cranial fossa).....	27
Figure 19: Section 2 (Anterior portion of middle cranial fossa) .....	28
Figure 20: Section 3 (Posterior portion of middle cranial fossa).....	28
Figure 21: Section 4 (Posterior cranial fossa) .....	29
Figure 22: Section 5 (Trigone of lateral ventricle) .....	29
Figure 23: Section 6 (Posterior to the occipital horn) .....	30
Figure 24: Midline sagittal section .....	30
Figure 25: Medial parasagittal view (Right and left) .....	31
Figure 26: Lateral parasagittal view (Right and left) .....	32
Figure 27: Posterior fontanelle sagittal view.....	32
Figure 28: Mastoid view .....	33
Figure 29: Periventricular echogenicity.....	34
Figure 30: Coronal and sagittal views showing localised periventricular echolucencies suggestive of periventricular leukomalacia .....	35
Figure 31: Coronal and sagittal views showing more extensive periventricular echolucencies suggestive of periventricular leukomalacia.....	36
Figure 32: Extensive frontoparietal periventricular leukomalacia .....	37
Figure 33: Grade 1 germinal matrix haemorrhage.....	38
Figure 34: Grade 2 IVH .....	39
Figure 35: Grade 2 IVH into occipital horn of lateral ventricle.....	40
Figure 36: Grade 3 IVH .....	41
Figure 37: Grade 4 IVH with midline shift .....	42

**References..... 43**

## A systematic approach to the documentation of cranial ultrasound findings

1. Demonstrate key anatomical structures in coronal and sagittal sections.
2. Evaluate the ventricular system.
3. Identify and report germinal matrix/ intraventricular/periventricular haemorrhage (GMH/IVH) and periventricular leukomalacia (PVL).
4. Evaluate the cerebrovascular system (anterior cerebral artery, middle cerebral artery, superior sagittal sinus).
5. Evaluate superficial convexity of the brain, including superficial lesions
6. Further evaluation of cerebral lesions, including congenital anomalies, artefacts and normal variants.

## Key anatomical structures of the brain parenchyma

- Identify key anatomical structures ([Table 1](#), [Table 2](#), [Table 3](#)) in different views.
- Comment on the echogenicity and homogeneity (Hyperechoic – suggestive of ischemia, ([Figure 1](#)) haemorrhage (Grade 4 bleed) ([Figure 2](#)), or calcification (Figure 3) ([Figure 3](#)); anechoic – suggestive of lytic lesions. Comment, especially on periventricular echogenicity in preterm infants ([Table 4](#)).
- Differentiate physiological periventricular blush from periventricular echogenicity ([Table 5](#)). Mild periventricular echogenicity is usually seen in preterm infants during the first few days after birth ("periventricular blush"). The echogenicity appearance is further accentuated in the peritrogonal area in the parasagittal section due to the anisotropic effect from the ultrasound beam hitting the periaxial white matter fibres at a 90-degree angle.

## Evaluation of the ventricular system

- Size and Symmetry – If enlarged on visual impression, perform objective measures of hydrocephalus (e.g., anterior horn width ([Figure 4](#)), thalamo-occipital distance ([Figure 5](#)), ventricular index ([Figure 6](#)), Normative values are available. However, serial measures demonstrating the trend are more valuable than absolute measurements.
- Presence or absence of echogenicity within the cavity of ventricles – suggestive of intraventricular haemorrhage ([Figure 4](#)).
- Presence or absence of echogenicity of the lining of the ventricular system ([Figure 4](#)) – Echogenicity of the ependymal lining of the ventricular wall is due to chemical ventriculitis secondary to the irritant blood products<sup>1</sup>
- Any midline shift ([Figure 7](#))

## Reporting of Germinal matrix/ intraventricular/periventricular haemorrhage (GMH/IVH) and periventricular leukomalacia (PVL).

GMH/IVH was described initially by Papile et al., based on a CT scan report in a cohort of 46 infants <1500 G<sup>2</sup>, and continues to be followed in many centres. Adherence to Papile's classification ([Table 6](#)) is fraught with variation in reporting<sup>3,4</sup>. For example, Papile defined grade 3 IVH as a ventricle distended with the blood contained in it. However, the ventricle is often distended with blood and cerebrospinal fluid (e.g., secondary to a small clot obstructing the aqueduct), which is included in the definition of a grade 3 IVH in some NICUs. Choroid plexus haemorrhage is considered either grade 1 or grade 2 or outside the current grading system. Grade 1 GMH can be over-reported, perhaps because it can be difficult to distinguish between germinal matrix congestion and haemorrhage. Similarly, issues may be faced with the grading system for PVL ([Table 4](#)).

A datasheet that describes the sonographic findings of IVH/PVL rather than any specific grading system may improve the consistency of reporting and reduce inter-observer variability. One such method was proposed by Harris et al.<sup>3</sup>. A modification of this system has been described in

### Evaluation of cerebrovascular system

- Document resistance index in the anterior cerebral artery ([Figure 8](#)) and middle cerebral artery ([Figure 9](#))
- Using a high-frequency transducer, perform Doppler to demonstrate venous flow within the superior sagittal sinus ([Figure 10](#)). The absence of flow indicates superior sagittal sinus thrombosis. ([Figure 11](#))
- Evaluate any other vascular anomalies (Eg: lenticulostriate vasculopathy ([Figure 12](#)), the vein of Galen A-V malformation)

### Evaluation of superficial convexity of the brain

Evaluate superficial convexities using a high-frequency transducer and comment on

#### Extra-axial space

Serial measurement of the width of the subarachnoid space is valuable. ([Figure 13](#)). In extremely preterm infants, the subarachnoid space may be wider soon after birth and gradually decrease because of brain growth and loss of fluid. Increasing subarachnoid space at term postmenstrual age may indicate impaired brain growth<sup>5</sup>.

#### Grey-white matter differentiation:

In a normal brain, well-defined hyperechoic pia mater overlies hypoechoic cortical grey matter, which in turn overlaps slightly hyperechoic white matter. ([Figure 13](#)) Generalised loss of grey-white matter differentiation with effacement of lateral ventricles is suggestive of cerebral oedema, typically seen in hypoxic-ischemic encephalopathy ([Figure 1](#)).<sup>9</sup>

## Artefacts and anatomical variants

- Asymmetrical lateral ventricle – Asymmetry of lateral ventricles is common<sup>10</sup>. Preservation of triangular configuration, larger ipsilateral choroid plexus, absence of echogenic ependymal lining/ IVH, and failure to demonstrate an increase in the size on follow-up scans are the clues suggesting normality<sup>10,11</sup>.
- Hyperechoic periventricular halos are often demonstrated in the parasagittal view, especially in the region above the trigonal area of the lateral ventricle. This is an artefact produced by the ultrasound beam that strikes the nerve fibres and blood vessels perpendicular to their course (anisotropic artefact). These are often relatively homogeneous with poorly defined margins, less echogenic than the adjacent choroid plexus, and not seen in other planes (e.g., scanning through posterior fontanelle).<sup>10,11</sup>  
([Figure 14](#))
- Diffuse, subtle, echogenic "haze" of the deep nuclei (ganglia and thalamus) can be a normal finding in extremely preterm infants. The echogenicity is seen within the first days of life and gradually normalises later.<sup>14,15</sup> Echogenicity with precise borders and visualised in at least two different planes suggest pathology. ([Figure 15](#))
- The choroid plexus generally has smooth and sharp margins ([Figure 15](#)) but sometimes has a bumpy contour or a cleft (giving a split appearance), which is suspicious of a layered clot. Vascularity on colour Doppler imaging and the absence of other signs of haemorrhage help distinguish from a clot due to intraventricular haemorrhage.<sup>5</sup>
- Choroid plexus cysts: Note the number and size. Multiple, bilateral, or larger than 1 cm choroid plexus cysts have been associated with chromosomal anomalies in some infants.<sup>11</sup>  
([Figure 16](#))

- Connatal cysts: Generally multiple (similar to a string of pearls) and bilaterally symmetric cysts located adjacent to the frontal horns just anterior to the foramina of Monro<sup>11</sup>. ([Figure 17](#))
- Care should be taken while evaluating the posterior fossa from the mastoid fontanelle because artefacts due to the cranial bones may be misinterpreted as cerebellar haemorrhage. By tilting the probe and scanning in a different view, the echogenicity disappears<sup>5</sup>.
- Coarctation of lateral ventricles – Focal approximation of the ventricular walls at any point medial to the external angle. When the approximation is complete, the external angle assumes a rounded configuration, simulating a cyst on the coronal view. This can be confused with germinolytic cysts or cystic periventricular leukomalacia<sup>10</sup>. Germinolytic cyst is located below the lateral ventricle, and cystic PVL is located above the external angle of the lateral ventricle. In contrast, coarctation is situated at the external angle of the lateral ventricle.
- A persistent fetal fluid-filled space located in the pineal region (just above the roof of the third ventricle) is termed a cavum veli interpositi and should not be confused with a congenital pineal region cyst or vein of Galen malformation<sup>12,13</sup>
- Mega Cisterna Magna<sup>11</sup>: The typical cisterna magna is less than 8 mm (typically 3-8 mm) in both the sagittal and axial planes. A mega cistern Magna is a normal variant. It is distinguished from an arachnoid cyst by its lack of mass effect and from a Dandy-Walker malformation by the presence of the cerebellar vermis.



## Tables

**Table 1: Standard view via anterior fontanel - Coronal sections**

Sections - Hall mark shape	Structures seen in different sections
<p>Section 1 (anterior cranial fossa): The base of the skull looks like the hull of a ship -due to the shape of the lesser wing of the sphenoid (Hill sign), and the orbitals look similar to a lemon (lemon sign) (<a href="#">Figure 18</a>)</p>	<p><b>Midline structures</b></p> <ul style="list-style-type: none"> <li>• Falx cerebri and interhemispheric fissure (anterior cerebral artery pulsations noted here)</li> <li>• Superior sagittal sinus - triangular-shaped structure with hyperechoic boundaries and hypoechoic lumen</li> <li>• Corpus callosum (rostrum, genu, body, and splenium)</li> <li>• Cavum septum pellucidum (seen inferior to the genu of the CC in at least 90% of all preterm neonates and 60% of full-term infants and closes 2-6 months after birth)<sup>1</sup></li> <li>• Foramen of Monro</li> <li>• Third ventricle – difficult to see or seen as a slit-like structure in the midline</li> <li>• Cerebellar vermis</li> <li>• Fourth ventricle and Cisterna magna (difficult to see)</li> </ul> <p><b>Para-midline structures</b></p> <ul style="list-style-type: none"> <li>• Frontal lobes</li> <li>• Anterior horns of lateral ventricles</li> <li>• Basal ganglia (caudate nucleus abutting and indenting lateral ventricles). Lateral to the caudate is the anterior limb of the internal capsule and the lentiform nucleus (comprised of globus pallidus medially and putamen laterally).</li> <li>• Thalamus on either side of 3<sup>rd</sup> ventricle</li> </ul> <p><b>Lateral structures</b></p> <ul style="list-style-type: none"> <li>• Frontal lobes</li> <li>• Temporal lobes</li> <li>• Parietal lobes</li> <li>• Occipital lobes</li> <li>• Sylvian fissures (lateral sulcus) – Y shaped in term infants – the pulsating branch of the middle cerebral artery is located in its depth (part of the cerebral cortex located deeper to the Sylvian fissure is called insula) and more squared (broader) in preterm infants</li> </ul>
<p>Section 2 (anterior portion of middle cranial fossa): (<a href="#">Figure 19</a>) The base of the skull has an echogenic mask-like appearance – resulting from the lesser wing of the sphenoid (upper portion of the mask) and greater wing of the sphenoid (lower portion of the mask).</p>	
<p>Section 3 (posterior portion of middle cranial fossa): (<a href="#">Figure 20</a>) The base of the skull maintains the squared-off shape of the temporal bone but starts to appear rounded at the middle, where the occipital bone starts to appear</p>	
<p>Section 4 (posterior cranial fossa): (<a href="#">Figure 21</a>)</p> <ul style="list-style-type: none"> <li>• The rounded appearance of the base of the skull – formed by the occipital bone.</li> <li>• "Dancing lady" appearance in the midline <ul style="list-style-type: none"> <li>▪ Tentorium cerebelli forms the imaginary skirt for the lady</li> <li>▪ The cerebellar vermis corresponds to the lower trunk</li> <li>▪ The quadrigeminal plate cistern corresponds to the upper trunk (the quadrigeminal plate or tectum is the dorsal part of the midbrain)</li> <li>▪ The choroid plexus correspond to the eyes</li> </ul> </li> </ul>	
<p>Section 5 (Trigone of the lateral ventricle): (<a href="#">Figure 22</a>)</p> <ul style="list-style-type: none"> <li>• The rounded appearance of the base of the skull – formed by the occipital bone.</li> <li>• Choroid plexus filling up the diverging lateral ventricles</li> </ul>	
<p>Section 6 (Posterior to the occipital horn): (<a href="#">Figure 23</a>)</p> <ul style="list-style-type: none"> <li>• The rounded appearance of the base of the skull – formed by the occipital bone</li> </ul>	

**Table 2: Standard view via anterior fontanel - Sagittal sections**

Sections - Hall mark shape	Structures seen in different sections
<p>Midline sagittal section: (<a href="#">Figure 24</a>)</p> <p>The base of the skull is formed by the clivus and appears straight. Occasionally it could appear like a staircase as a result of the uneven ossification of the clivus</p>	<ul style="list-style-type: none"> <li>• The superior sagittal sinus</li> <li>• Cingulate gyrus (cingulate sulcus superiorly and callosal sulcus inferiorly)</li> <li>• Corpus callosum – hypoechoic structure (genu, body, and splenium from anterior to posterior)</li> <li>• Cavum septum pellucidum</li> <li>• Massa intermedia (thalamic adhesion)</li> <li>• 3<sup>rd</sup> ventricle</li> <li>• 4<sup>th</sup> ventricle lies inferior and posterior to 3<sup>rd</sup> ventricle</li> <li>• The brain stem (pons) anterior to the 4<sup>th</sup> ventricle</li> <li>• Cerebellar vermis – posterior to 4<sup>th</sup> ventricle</li> <li>• Cisterna magna posterior and inferior to 4<sup>th</sup> ventricle</li> </ul>
<p>Medial parasagittal view (Right and left): (<a href="#">Figure 25</a>)</p> <p>The base of the skull has a scalloped configuration due to the combination of the anteriorly located sphenoid bone and the more posteriorly located temporal bone</p>	<ul style="list-style-type: none"> <li>• Lateral ventricle (frontal horn, body, atrium, occipital horn, and temporal horn). Temporal horn – may not be clearly visualised unless dilated.</li> <li>• Basal ganglia</li> <li>• Thalamus</li> <li>• Caudothalamic groove - sonographic (not an anatomic) "groove" formed by the junction of the relatively hypoechoic head of the caudate nucleus and hyperechoic thalamus.</li> <li>• Choroid plexus</li> </ul>
<p>Lateral parasagittal view (Right and left): (<a href="#">Figure 26</a>)</p> <p>The base of the skull is rounded due to the temporal bone</p>	<p>Frontal and temporoparietal lobes of the brain.</p> <p>The angulation of the probe should be sufficient to include the Sylvian fissure and insula on each side.</p>

**Table 3: Supplemental views16-19**

Several supplemental views have been used. The most common application include

- Diagnosis of occipital horn bleed via posterior fontanel sagittal and parasagittal views. The occipital horn is devoid of choroid plexus. ([Figure 27](#)) Echogenicity within the occipital horns is indicative of intraventricular haemorrhage. ([Figure 35](#))
- Diagnosis of intracerebellar bleed by placing the transducer along the axial planes via mastoid fontanelle. ([Figure 28](#))
- Middle cerebral artery Doppler using temporal window ([Figure 9](#))

<b>Supplemental views</b>	<b>Structures seen</b>
Posterior fontanelle - <b>midline sagittal view</b>	<ul style="list-style-type: none"> <li>• Ventricular system (Occipital horn, trigone, and sometimes anterior and lateral horns of lateral ventricles)</li> <li>• Vermis</li> <li>• Fourth ventricle</li> <li>• peri cerebellar cisterns</li> <li>• pons and medulla</li> </ul>
Posterior fontanelle - <b>parasagittal views</b>	<ul style="list-style-type: none"> <li>• A choroid glomus, its two anterior extensions into the ventricular body and temporal horn</li> <li>• Occipital horns of the lateral ventricles</li> <li>• Occipital parenchyma</li> </ul>
Posterior fontanelle – <b>coronal view</b>	<ul style="list-style-type: none"> <li>• The most superior coronal view - the lateral ventricles with the choroid plexus and parts of the parietal and occipital lobes.</li> <li>• The middle and inferior coronal views - occipital horns, occipital lobes, tentorium, vermis, and cerebellar hemispheres</li> </ul>
Temporal Windows	<ul style="list-style-type: none"> <li>• Middle cerebral artery</li> <li>• Thalami - hypoechoic, inverted heart-shaped structure</li> <li>• Midbrain - hypoechoic lenticular structures contiguous with and immediately caudal to the thalami.</li> <li>• Third ventricle - anechoic, slit-like cleft between the thalami.</li> </ul>

	<ul style="list-style-type: none"> <li>• Aqueduct of Sylvius - echogenic line / thin, anechoic slit in the midbrain.</li> <li>• Perimesencephalic cistern and quadrigeminal cistern.</li> </ul>
<p>Mastoid Fontanelles (posterior fossa view) Located at the junction of posterior parietal, temporal, and occipital bones</p>	<ul style="list-style-type: none"> <li>• Pons and prepontine cistern</li> <li>• Fourth ventricle – seen within the brain stem and anterior to vermis in the more caudally angled US image obtained through the mastoid fontanelles</li> <li>• Vermis - echogenic midline structure posterior to the fourth ventricle and anterior to the anechoic cisterna magna</li> <li>• Cisterna magna - anechoic, semilunar midline space located posterior to the cerebellum.</li> <li>• Cerebellar hemispheres - ovoid, hypoechoic lateral masses containing linear parallel bright echogenicities, seen on either side of the vermis.</li> <li>• Transcerebellar diameter has been correlated with gestational age.<sup>20</sup></li> <li>• Tentorium - echogenic, linear meningeal folds seen on either side of the cerebellar hemisphere</li> <li>• Both the transverse and sigmoid sinuses can be seen.</li> <li>• The foramen of Magendie can sometimes be visualised at the inferior portion of the cerebellum as a linear or tubular echoless area extending between the fourth ventricle and the cisterna magna. This is seen most often in younger premature neonates.</li> </ul>

**Table 4: The ultrasound grading system for PVL has been described as follows<sup>21</sup>**

<b>Grade</b>	<b>Description</b>	<b>Ultrasound findings</b>
I	Periventricular densities, persisting for $\geq 7$ days ( <a href="#">Figure 29</a> )	<ul style="list-style-type: none"> <li>Echodensities seen in the region above the external angle of the lateral ventricle.</li> <li>Grade 1 PVL must be differentiated from a physiological periventricular flare.</li> <li>Avoid scanning with lower frequency transducers (e.g., 5 MHz) to over-diagnose hyperechogenicity.</li> <li>Optimise gain and TGC.</li> </ul>
II	Localised periventricular cysts ( <a href="#">Figure 30</a> )	<p>Scanning within an area of flare using a high-frequency probe is necessary to detect microcysts.</p> <p>Grade 2 PVL must be differentiated from</p> <ul style="list-style-type: none"> <li>Paraventricular frontal Germinolytic cysts</li> <li>Paraventricular porencephalic cysts, often secondary to grade 4 intraventricular bleed</li> </ul>
III	Extensive fronto-parieto-occipital periventricular cystic lesions (cystic periventricular leukomalacia) ( <a href="#">Figure 31</a> ) ( <a href="#">Figure 32</a> )	<p>The cysts are typically anechoic with a variably thick rim of echogenicity, giving a "Swiss cheese" appearance.</p> <p>Determine the location, number, and size of the largest cyst.</p>
IV	Extensive cystic lesions in the subcortical white matter (cystic subcortical leukomalacia)	In more mature preterm infants and term infants, the vulnerable area shifts to a more peripheral region, so PVL occurs in white matter adjacent to the floor of the sulci. Cysts are generally larger and less likely to resolve.

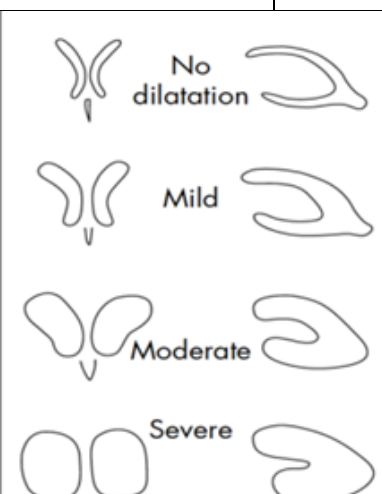
**Table 5: Differentiating physiological periventricular blush from PVL**

Physiological periventricular blush ( <a href="#">Figure 14</a> )	Mild PVL
<ul style="list-style-type: none"> <li>• Homogenous</li> <li>• Bilateral and symmetrical</li> <li>• Echogenicity is less than choroid plexus echogenicity</li> <li>• Some radial striations are seen</li> <li>• Vague margins</li> <li>• Becomes less conspicuous in other planes (e.g., images obtained via occipital fontanelle avoid anisotropy due to ultrasound beam insonated along the direction of nerve fibres)</li> <li>• Follow-up image – echogenicity becomes less prominent over the next 1-2 weeks. This is the only definitive way to differentiate it from PVL.</li> </ul>	<ul style="list-style-type: none"> <li>• Patchy with nodular accent</li> <li>• Usually unilateral/asymmetrical</li> <li>• Echogenicity matches or exceeds the choroid plexus echogenicity. However, the corollary is not necessarily true. This is because the choroid plexus is highly perfused in preterm infants. The more preterm an infant, the more echogenic the choroid plexus appears to be.</li> <li>• No radial striations</li> <li>• Sharp margins</li> <li>• Persists in different planes (In general, cerebral anomalies or injury should be visualised in at least two different planes)</li> <li>• Follow-up image – echogenicity persists, and eventually, cysts may develop. A persistence of flare beyond 7-14 days is considered suspicious of being abnormal and indicative of damage.</li> </ul>

**Table 6: Papile's classification of GMH/IVH**

	<b>Pathology</b>	<b>Ultrasound findings</b>
<b>Grade 1</b> ( <a href="#">Figure 33</a> )	Isolated subependymal haemorrhage confined to germinal matrix	Echogenicity in the subependymal region at the caudothalamic notch
<b>Grade 2</b> ( <a href="#">Figure 34</a> ) and ( <a href="#">Figure 35</a> )	Intraventricular haemorrhage without ventricular dilatation	Echogenicity extending into the anterior horn (anterior to Foramen of Monro) and/or occipital horn of lateral ventricles
<b>Grade 3</b> ( <a href="#">Figure 36</a> )	Ventricles filled with blood and dilated	Dilated ventricles assessed subjectively as well as objective measures
<b>Grade 4</b> ( <a href="#">Figure 37</a> )	Intraventricular haemorrhage extending into the brain parenchyma	Echogenicity with a definite margin in the periventricular area and associated with intraventricular echogenicity

**Table 7: Proposed modification from Harris et al. <sup>3</sup> describing GMH/IVH**

Ventricles	Blood in the subependymal region	No	Yes - R / L / both
	Blood in ventricle	No	Yes - R / L / both
	Size of ventricles	Normal	<ul style="list-style-type: none"> <li>• Distended - R / L / both</li> <li>• Distended with Blood / Blood and CSF</li> </ul>
	Lateral ventricle size at F. Monroe	Normal	Mild / Moderate / Severe dilatation
	Midline shift	No	Yes (shifted to right / shifted to left )
Parenchyma	Periventricular echogenicity (especially early echogenicity) in association with IVH (likely represents blood in parenchyma)	No	<ul style="list-style-type: none"> <li>• Yes - R / L / both</li> <li>• Location –</li> <li>• Size –</li> </ul>
	Periventricular echogenicity (especially late echogenicity) not associated with IVH (likely represents PVL)	No	<ul style="list-style-type: none"> <li>• Yes - R / L / both</li> <li>• Location –</li> <li>• Size –</li> </ul>
	Cysts in parenchyma	No	<ul style="list-style-type: none"> <li>• Yes - R / L / both</li> <li>• Location –</li> <li>• Number</li> <li>• Size of the largest cyst</li> </ul>
			



## Figures

Figure 1: Coronal section showing hyperechoic basal ganglia suggestive of ischaemia and effaced ventricles suggestive of cerebral oedema

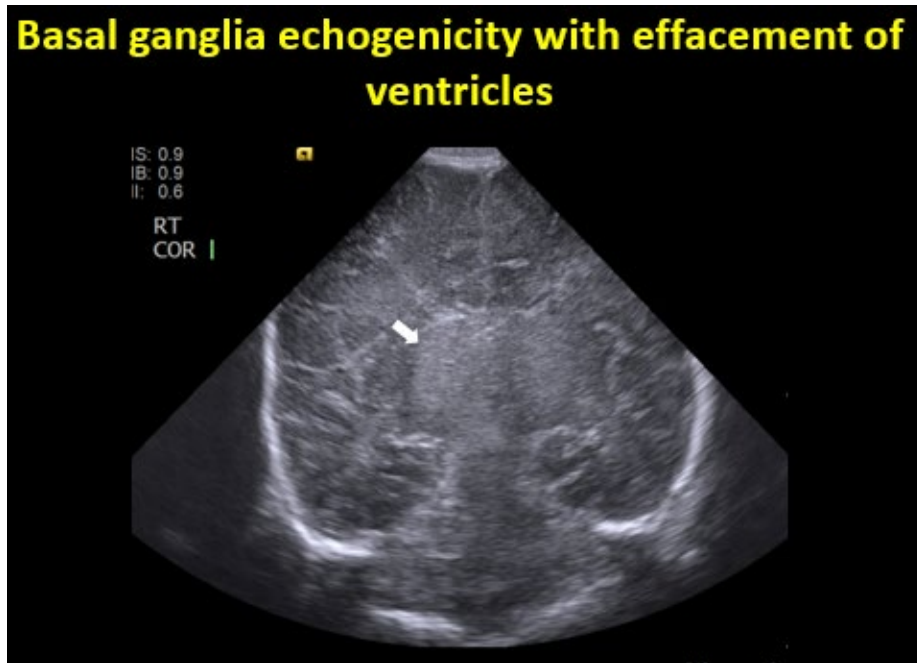


Figure 2: Parasagittal section showing hyperechoic parieto-occipital region suggestive of haemorrhage

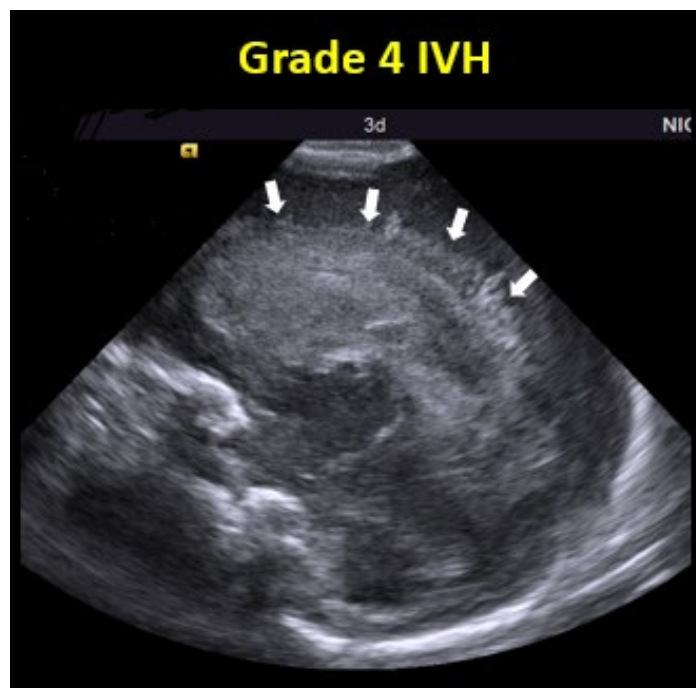


Figure 3: Coronal section showing hyperechoic spots (periventricular calcification)

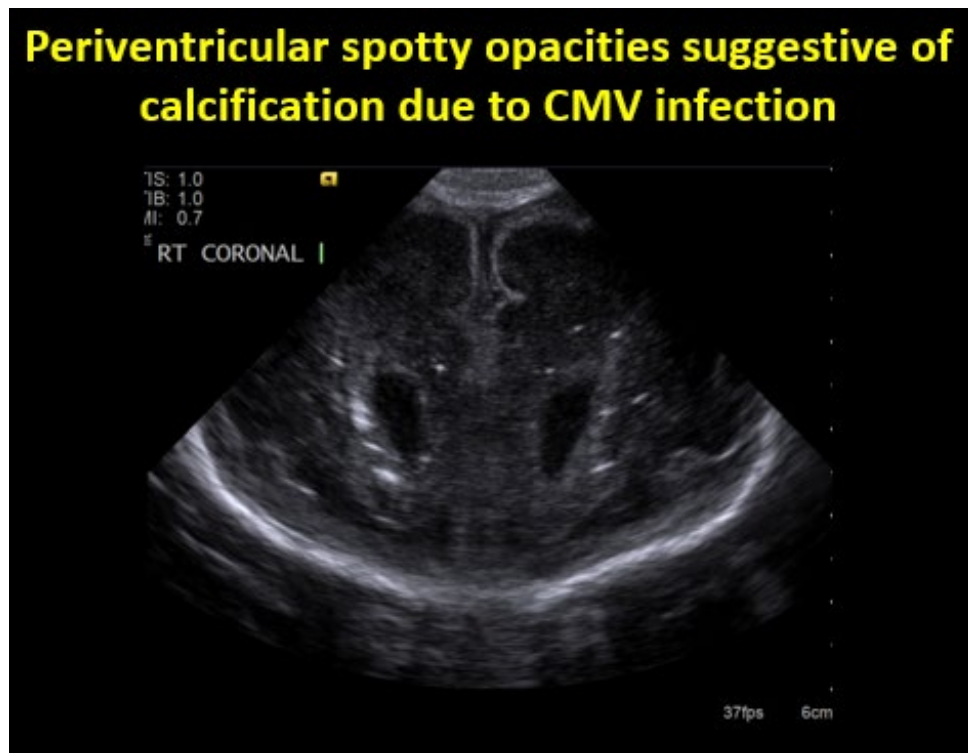
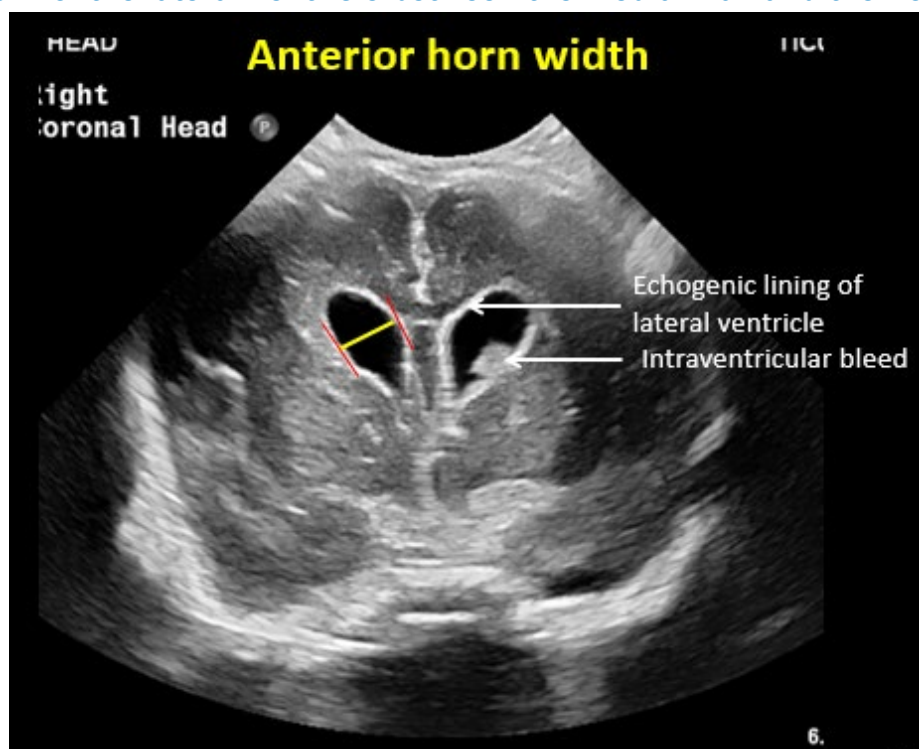
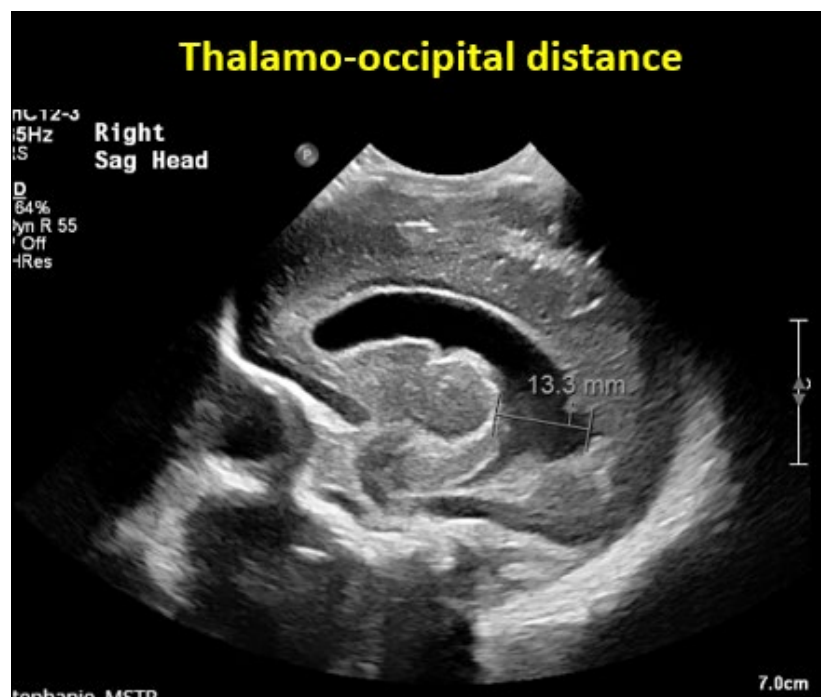


Figure 4: Coronal section at Foramen of Monro showing the widest distance of the anterior horn of the lateral ventricle between the medial wall and the floor



**Figure 5: Parasagittal view demonstrating maximum distance between the outermost point of the thalamus at its junction with the choroid plexus, and the outermost part of the occipital horn**



**Figure 6: Coronal section at Foramen of Monro showing the widest distance between the frontal horns (lateral to the lateral wall) at the level of the interventricular foramina of Monro**

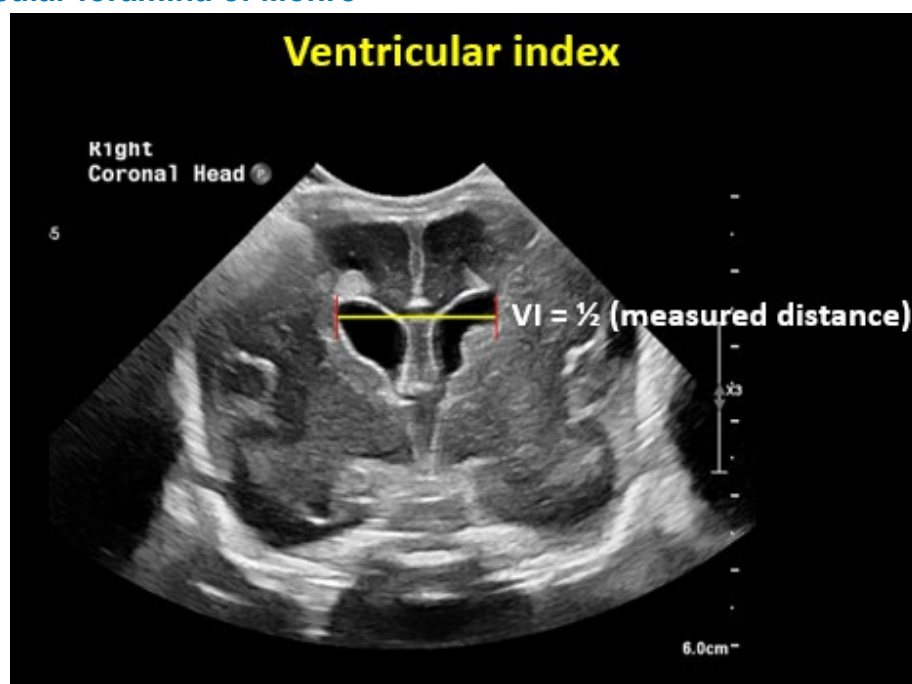


Figure 7: Coronal section showing a large intraventricular haemorrhage with midline shift

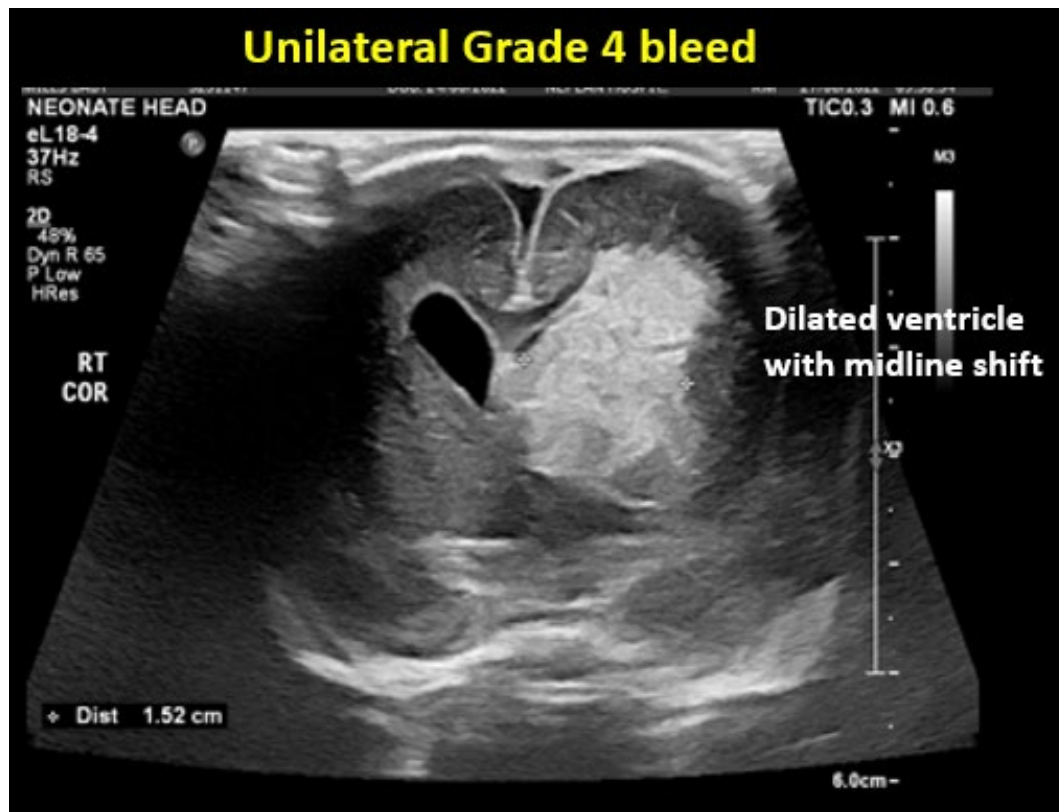


Figure 8: Midline sagittal section demonstrating anterior cerebral artery Doppler

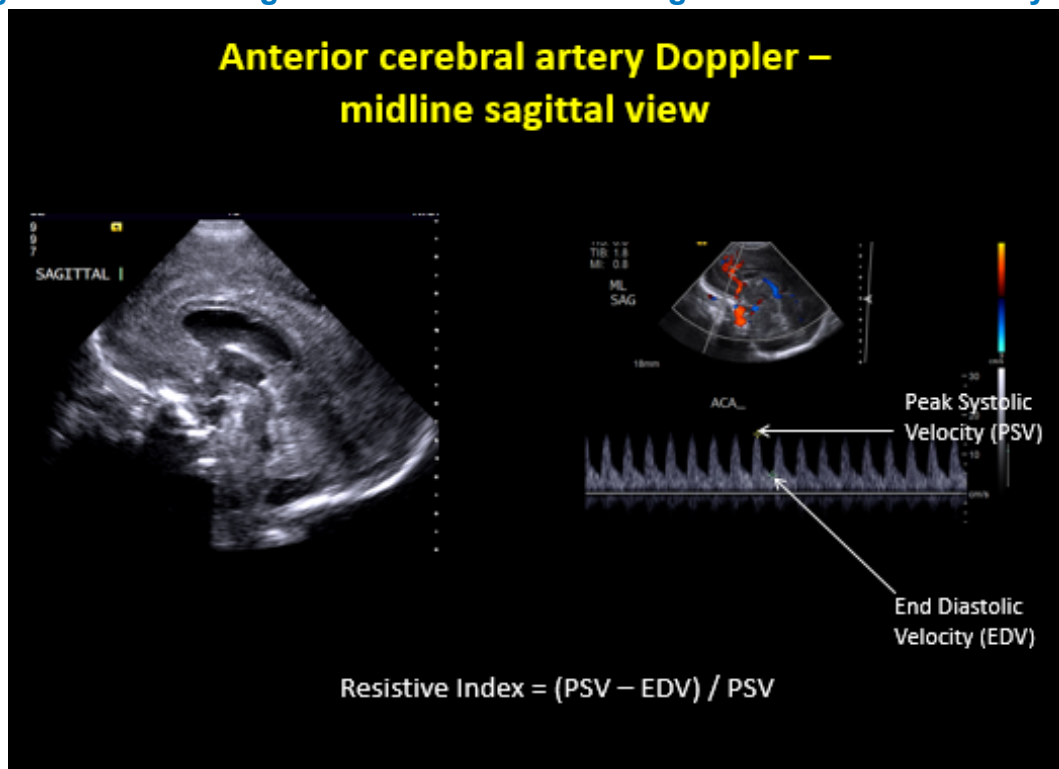
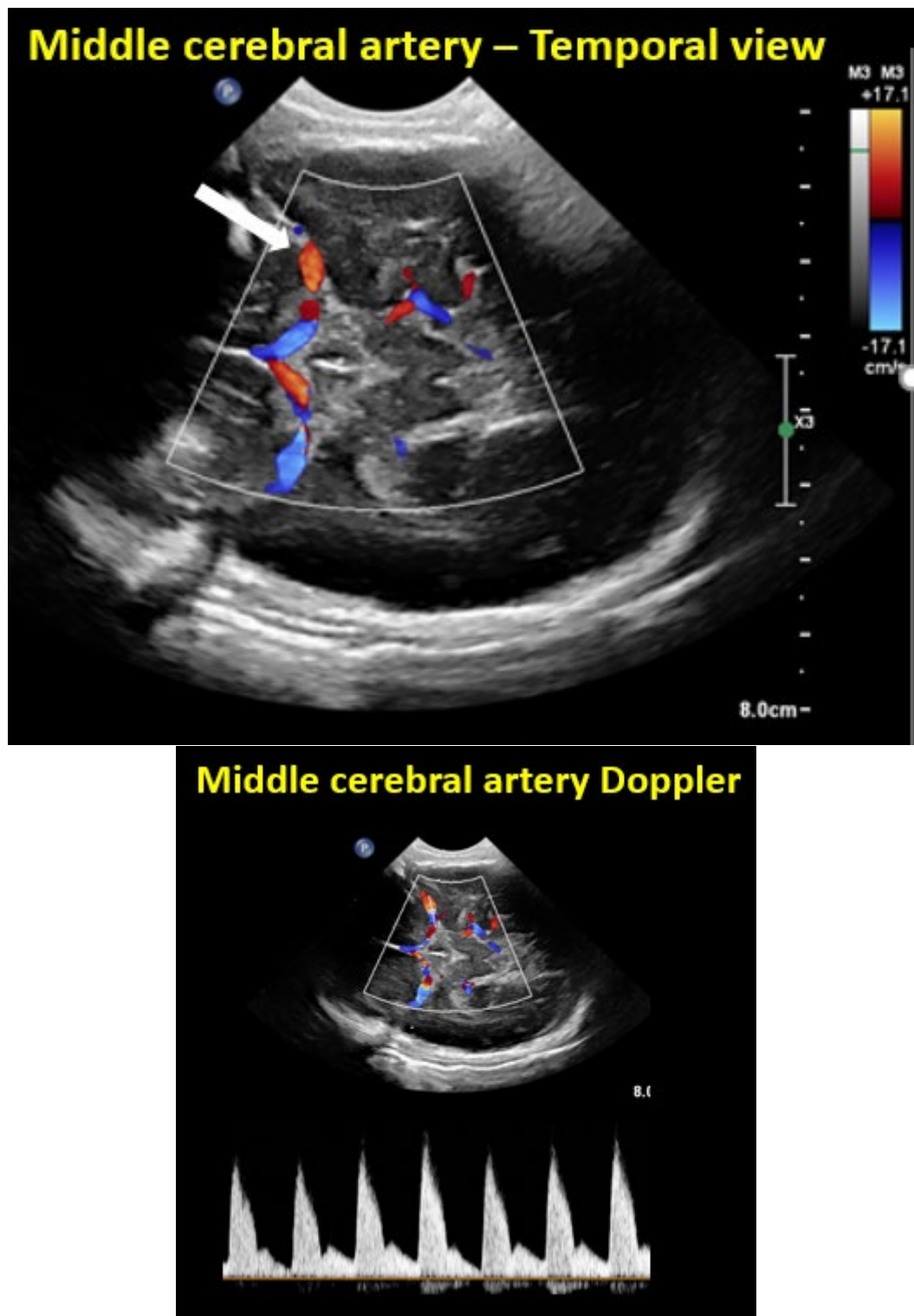


Figure 9: Temporal view demonstrating middle cerebral artery Doppler





**Figure 10: Sagittal and coronal section using high frequency transducer to demonstrate superior sagittal sinus flow**

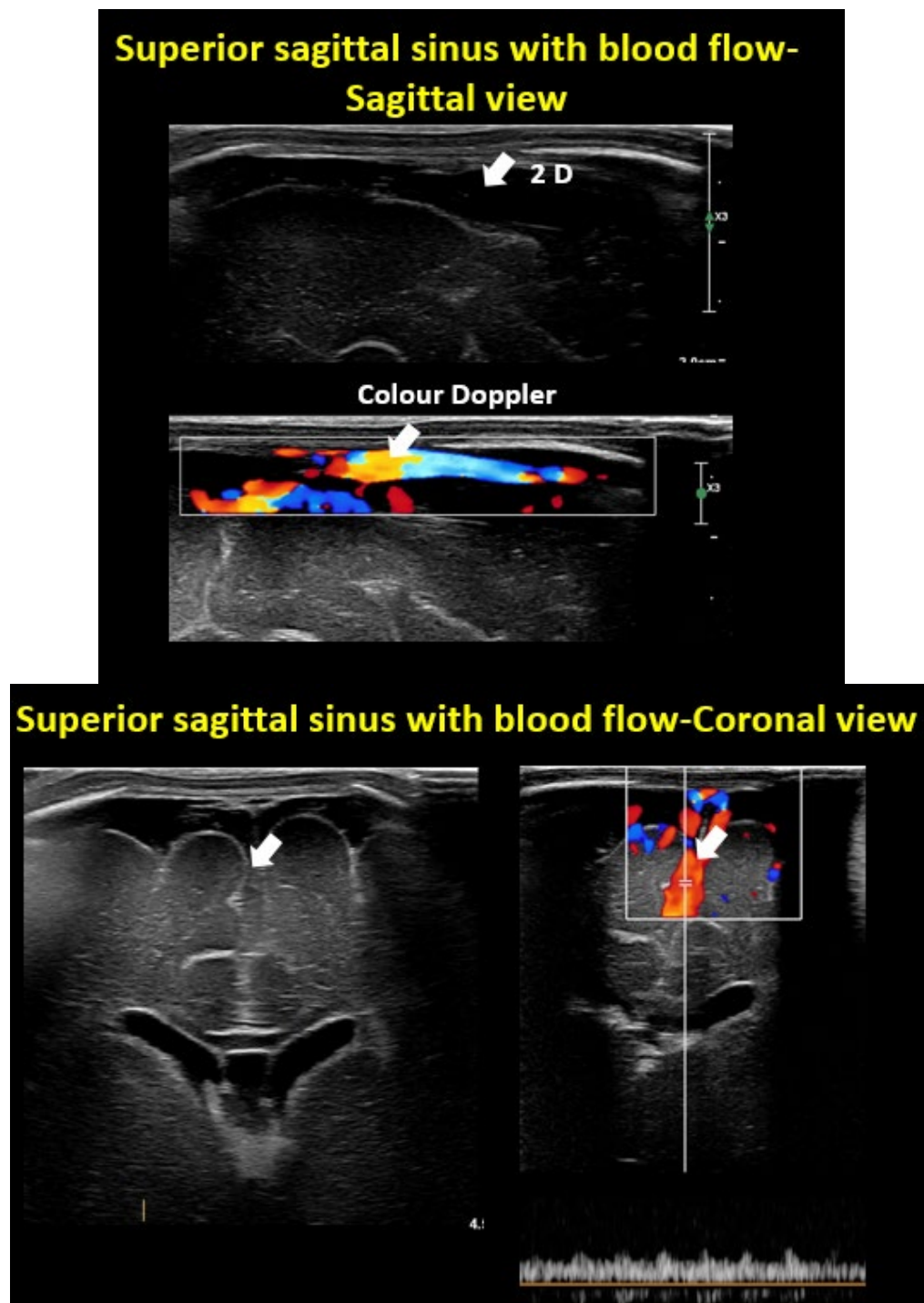
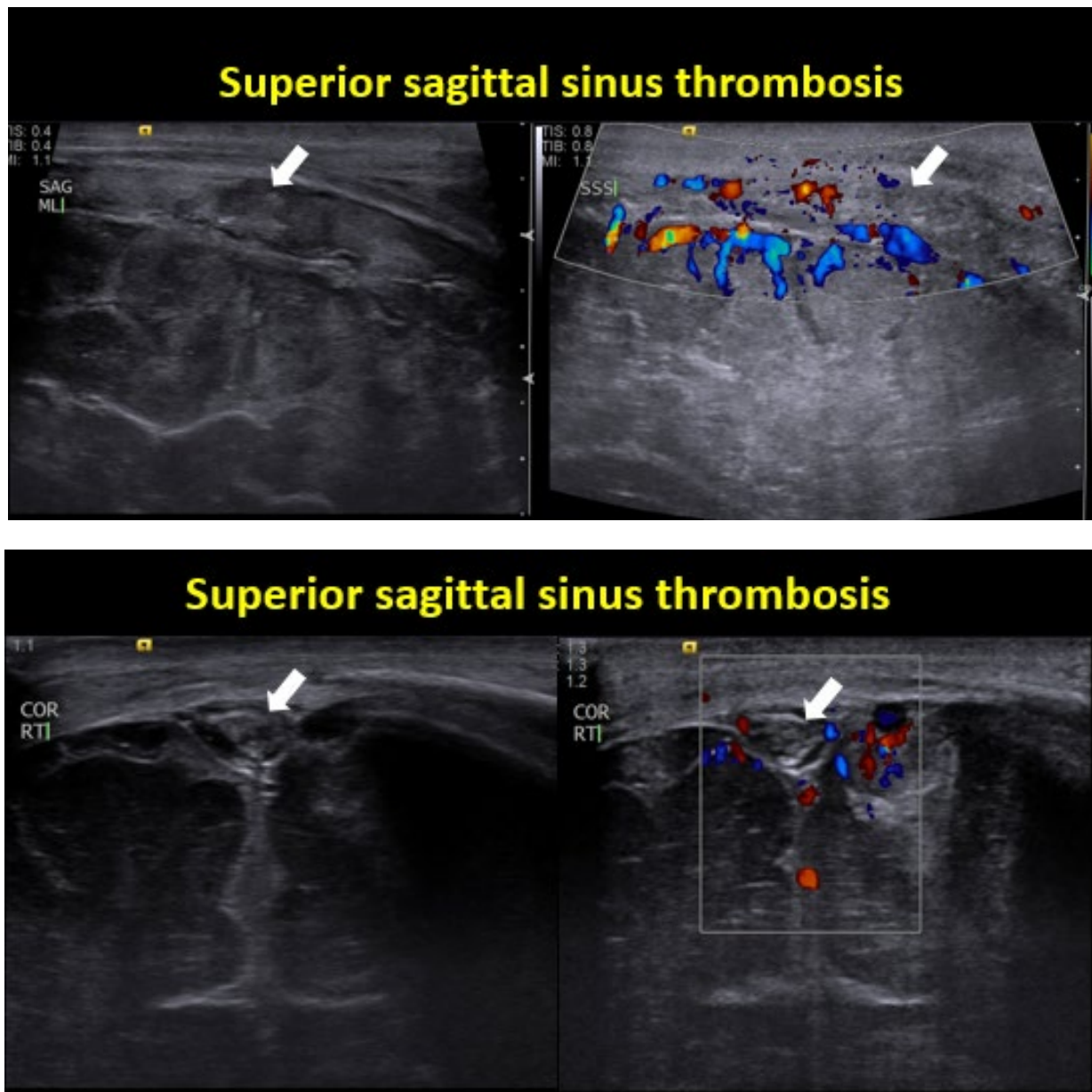
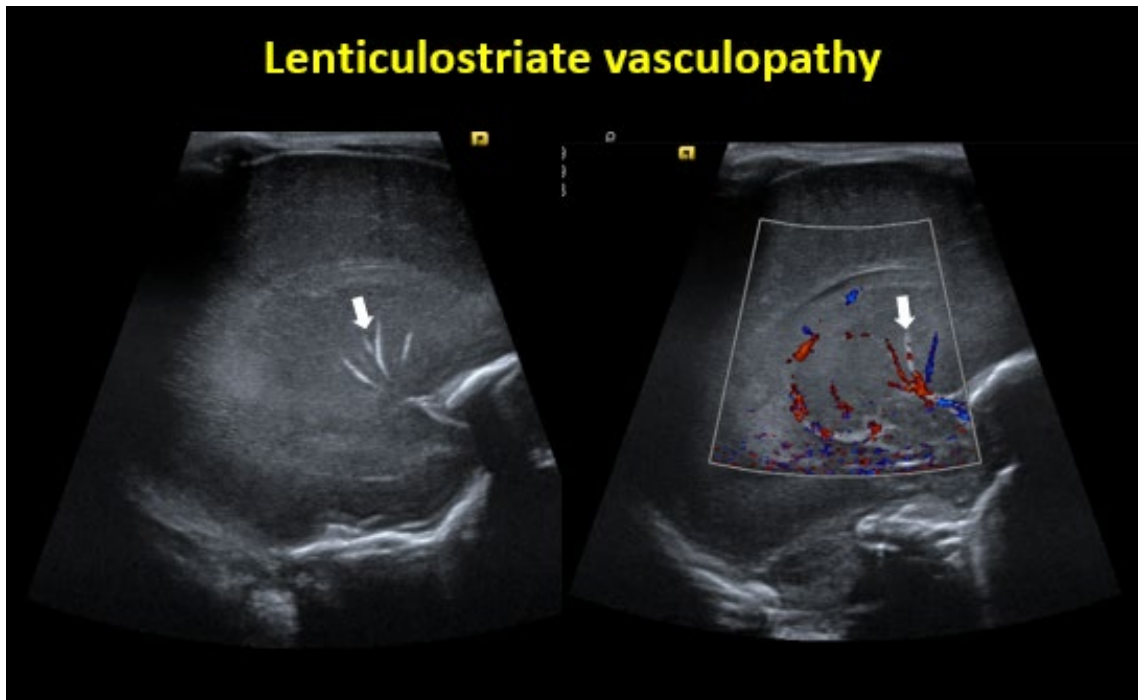


Figure 11: Sagittal and coronal section using high frequency transducer to demonstrate superior sagittal sinus thrombosis



**Figure 12: Parasagittal section demonstrating lenticulostriate vasculopathy in 2D and colour Doppler**



**Figure 13: Coronal section using high frequency transducer**





**Figure 14: Coronal and sagittal sections showing hyperechoic periventricular halos showing radial striations**

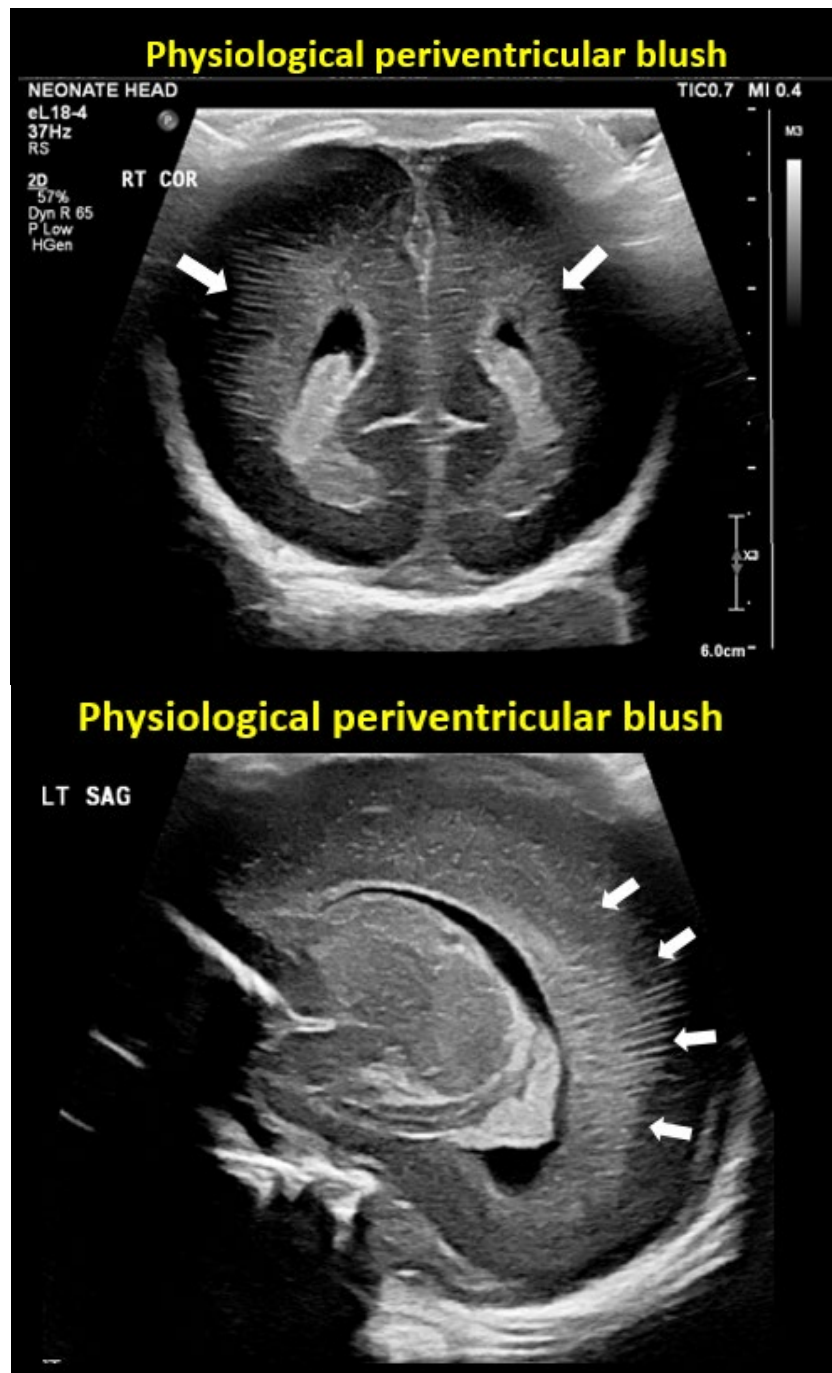


**Figure 15: Diffuse, subtle, echogenic haze of the deep nuclei can be a normal finding in extremely preterm infants**

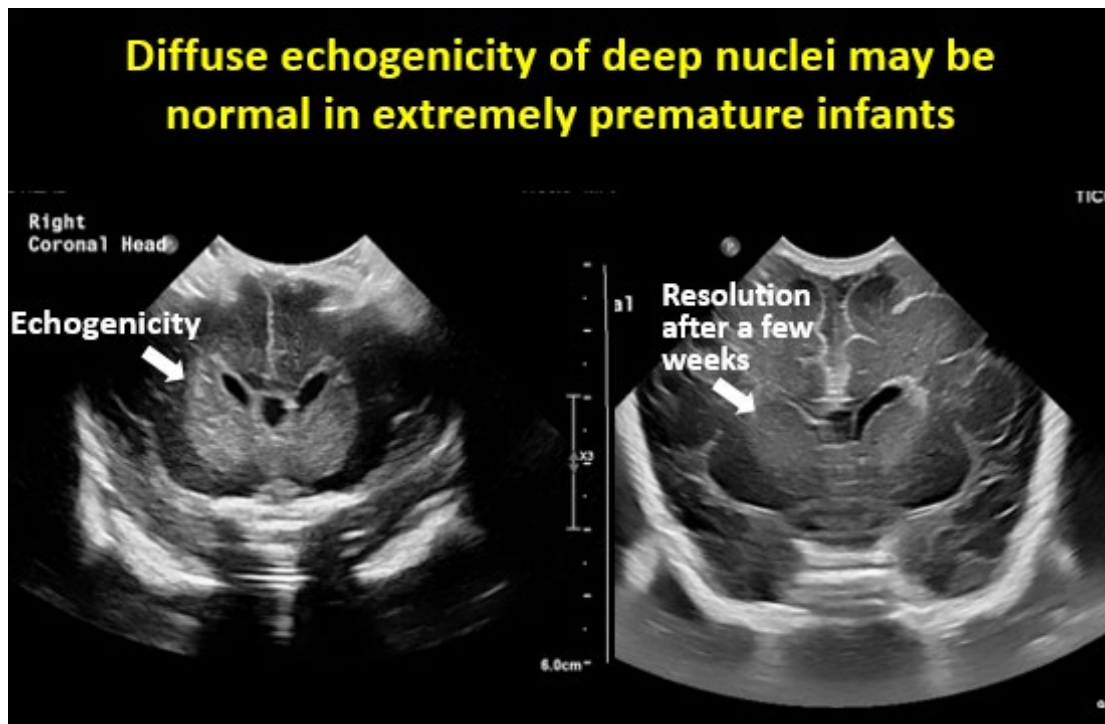


**Figure 16: Parasagittal view showing choroid plexus cyst**

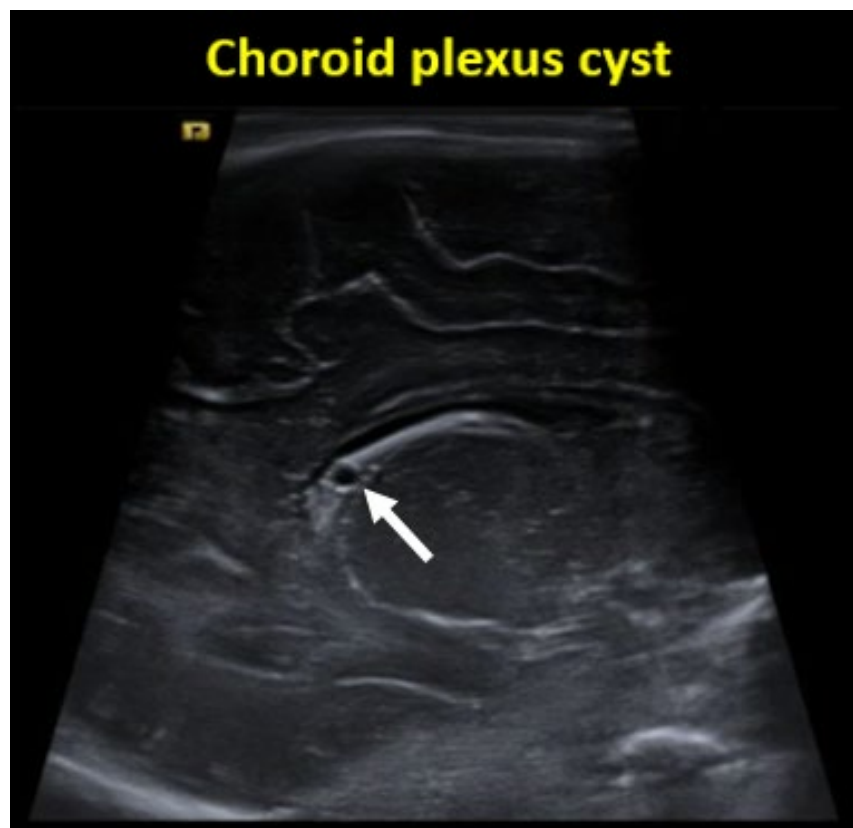


Figure 17: Parasagittal view showing connatal cysts

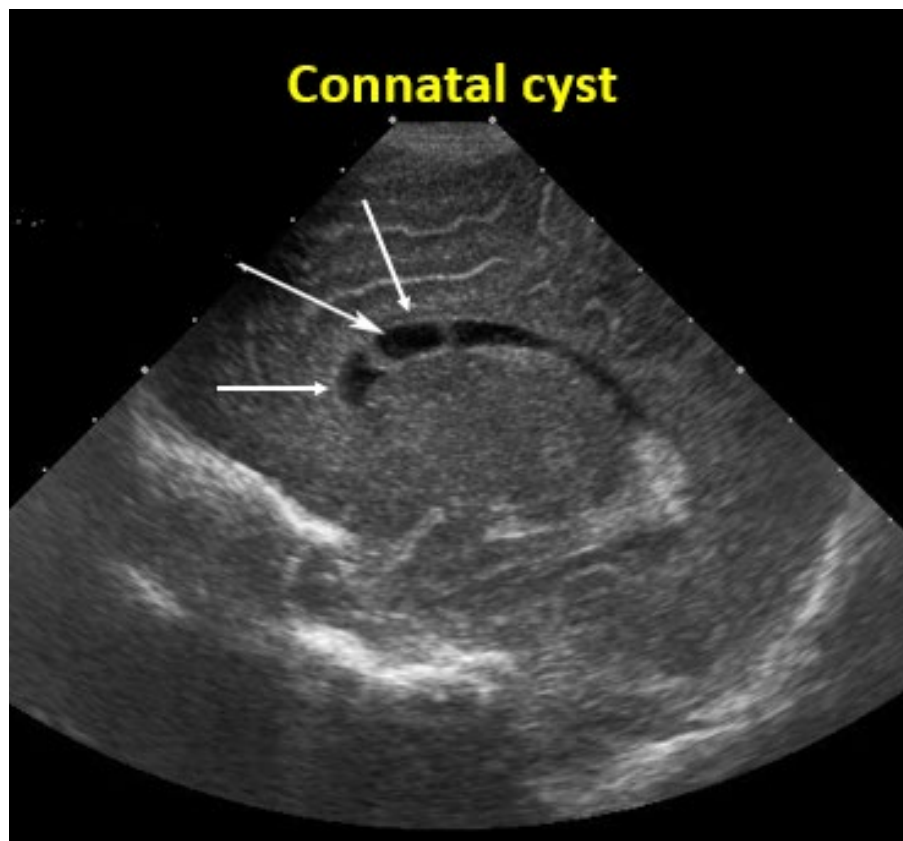


Figure 18: Section 1 (anterior cranial fossa)

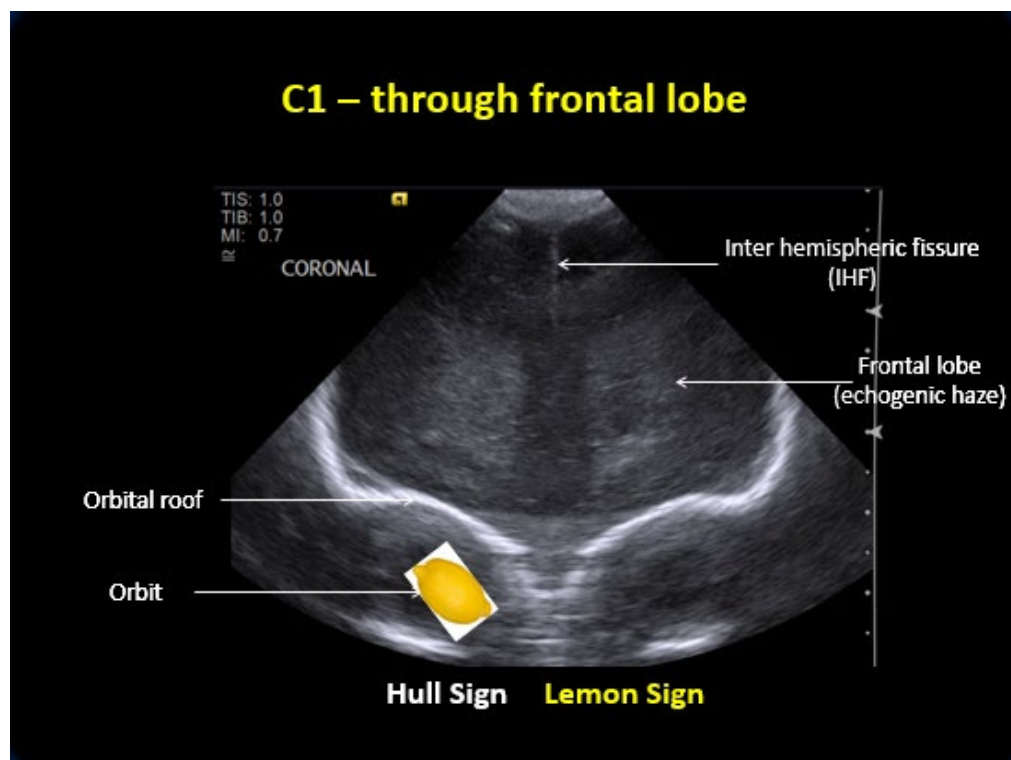


Figure 19: Section 2 (Anterior portion of middle cranial fossa)

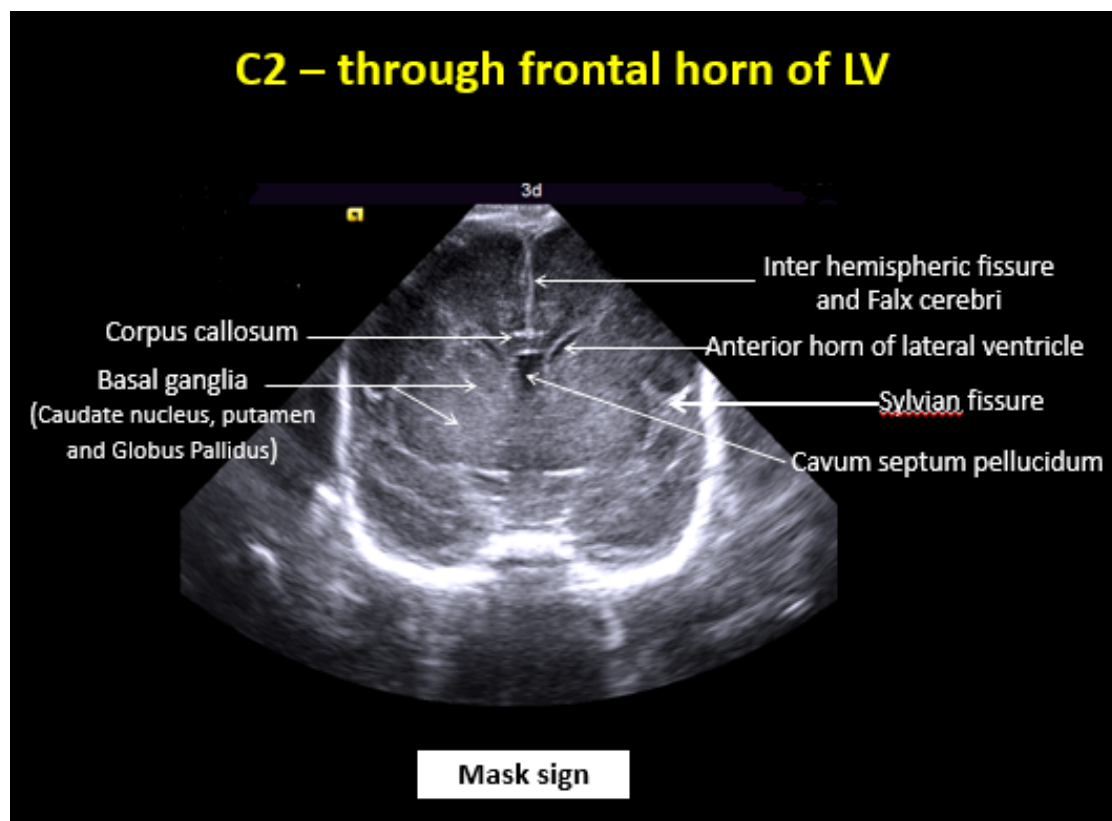


Figure 20: Section 3 (Posterior portion of middle cranial fossa)

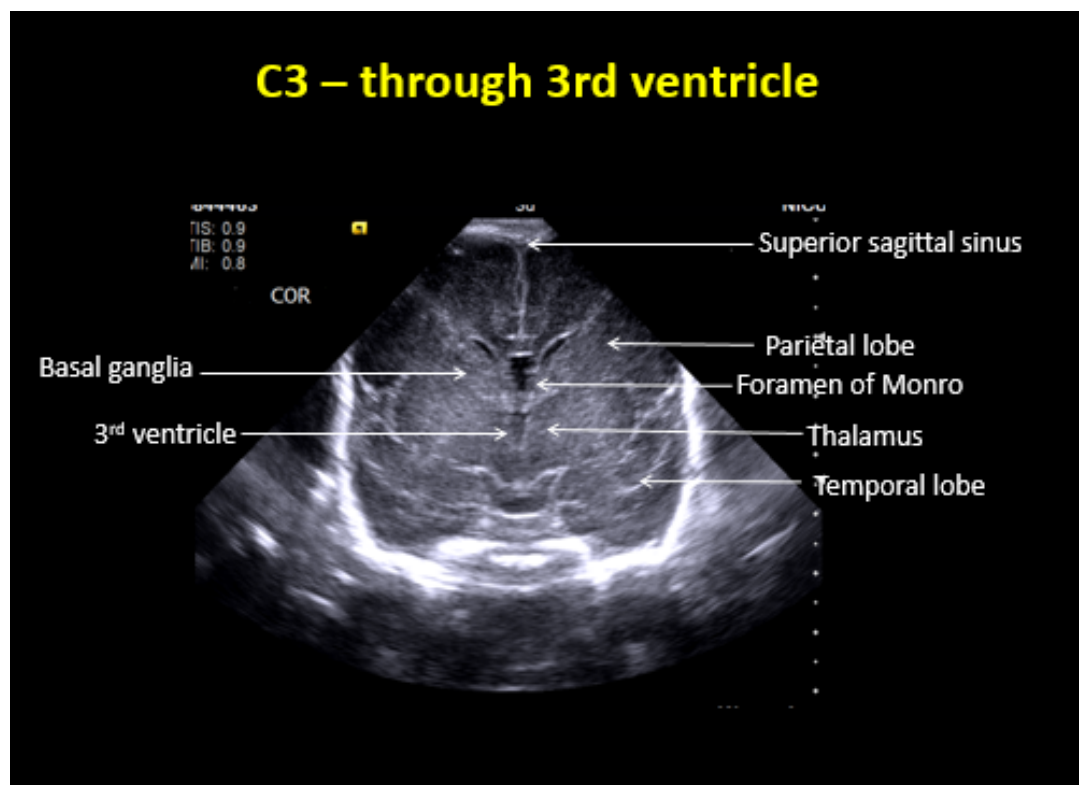


Figure 21: Section 4 (Posterior cranial fossa)

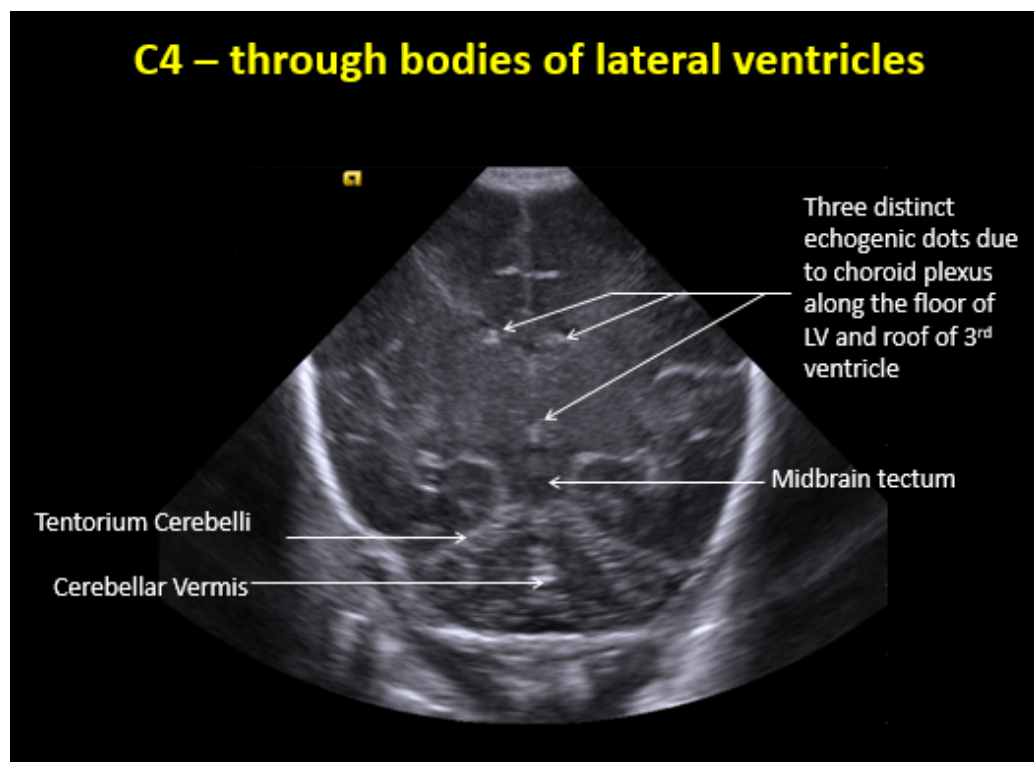


Figure 22: Section 5 (Trigone of lateral ventricle)

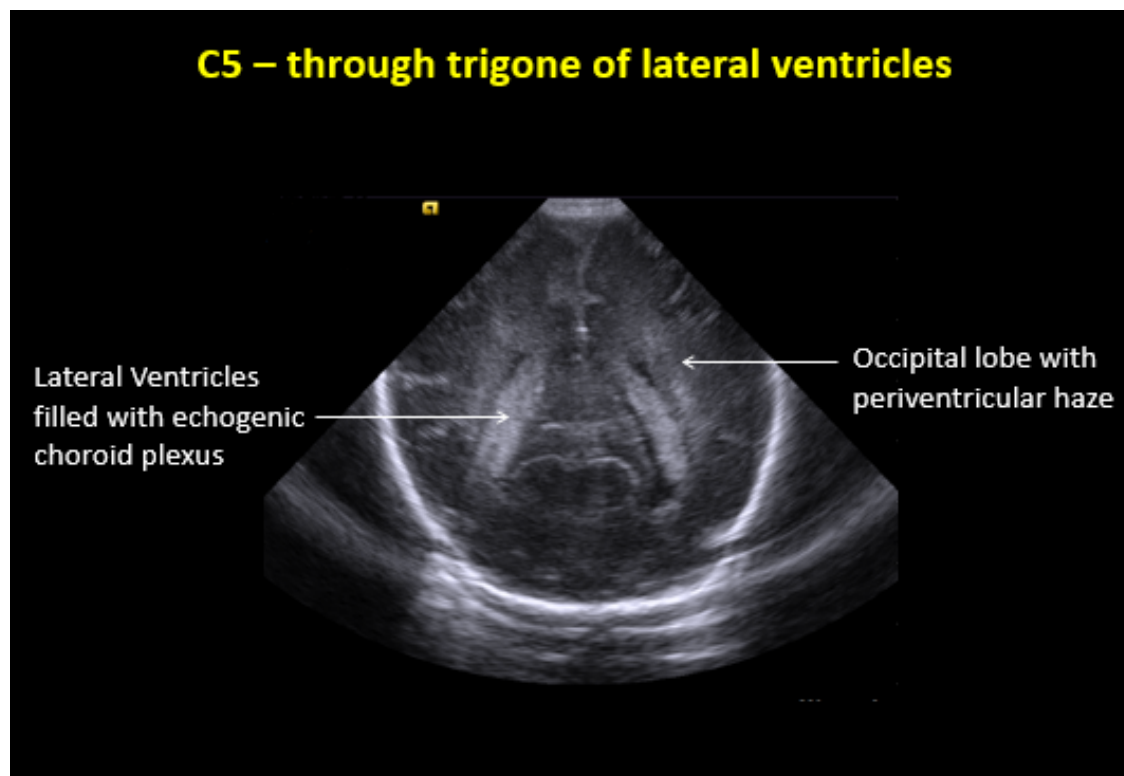




Figure 23: Section 6 (Posterior to the occipital horn)

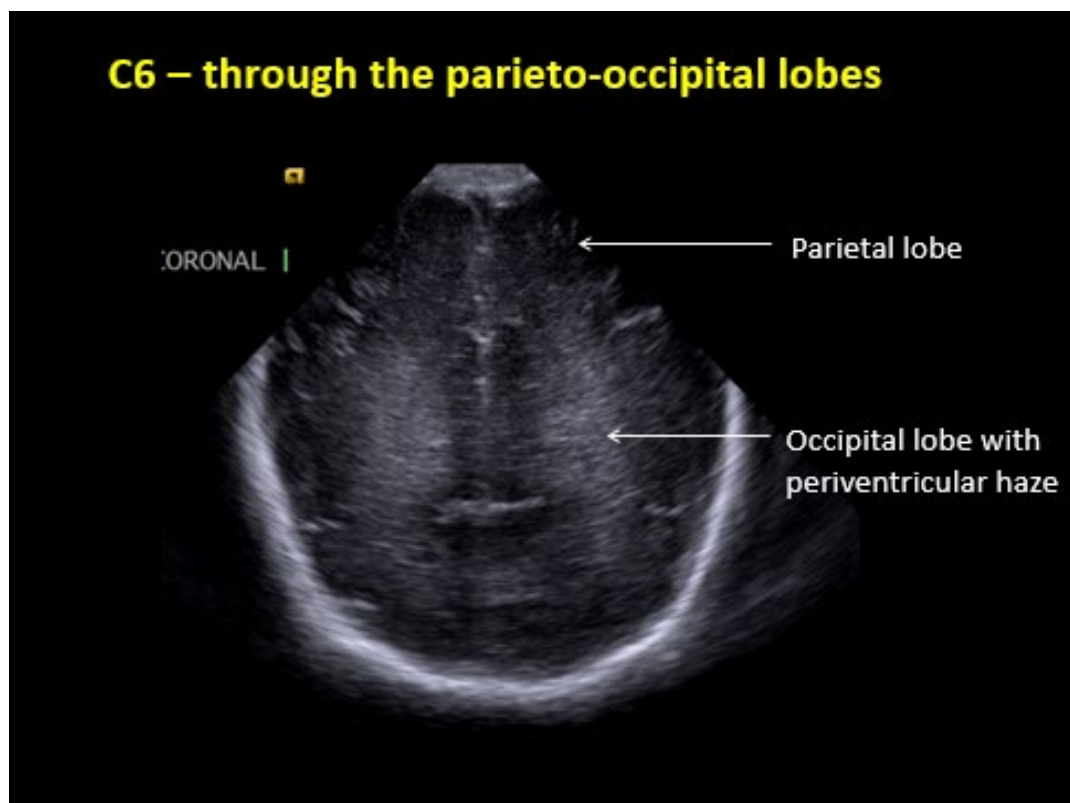
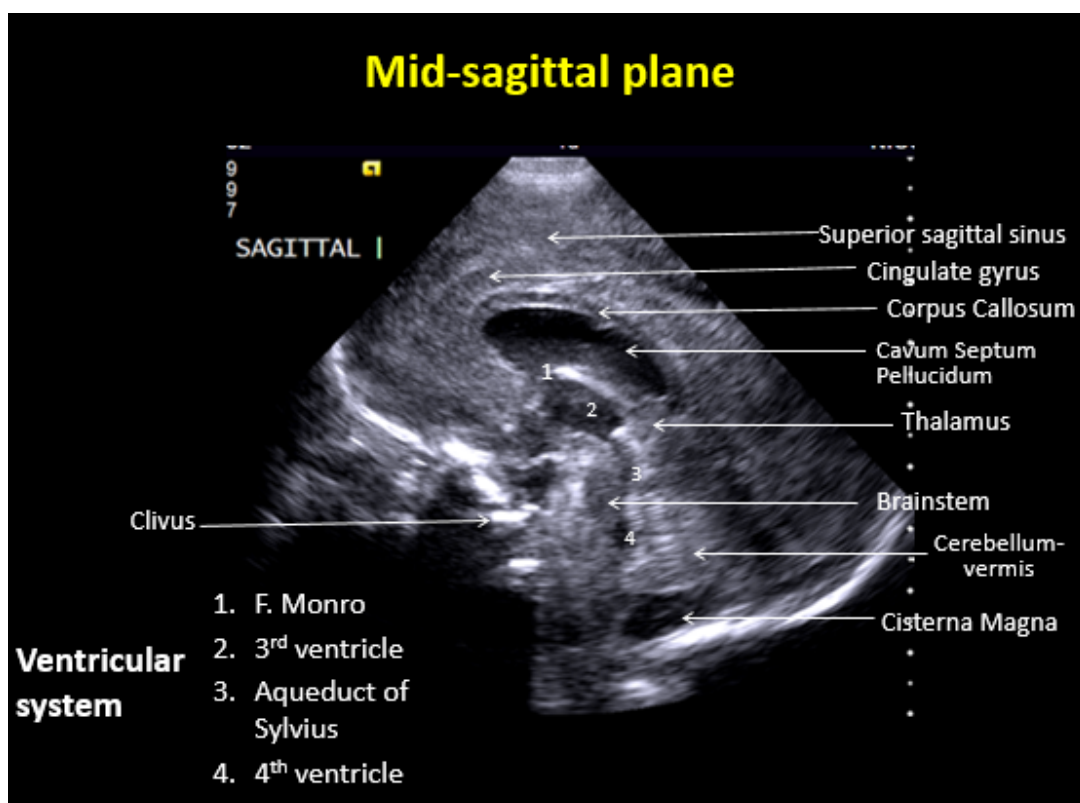


Figure 24: Midline sagittal section



**Figure 25: Medial parasagittal view (Right and left)**

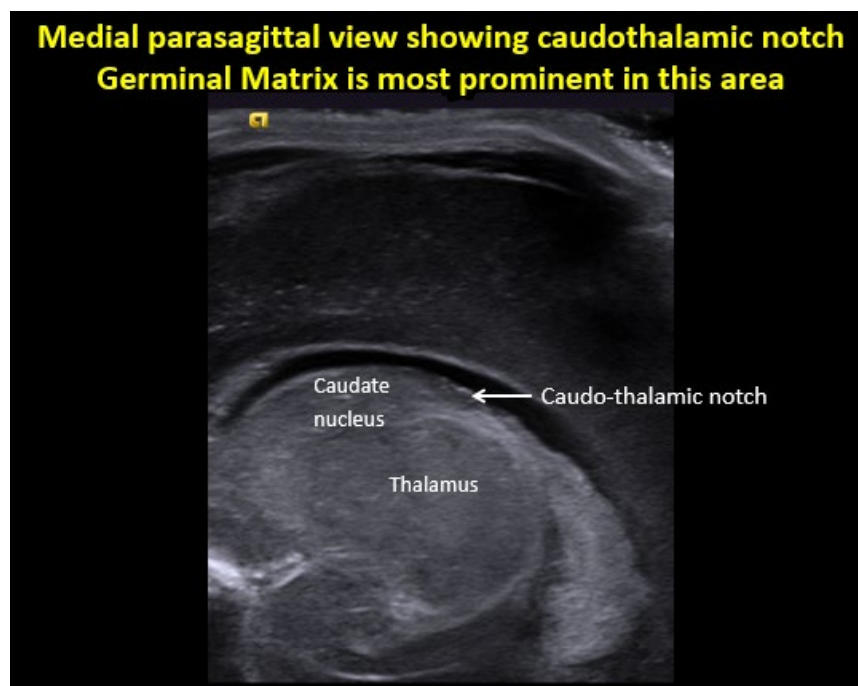
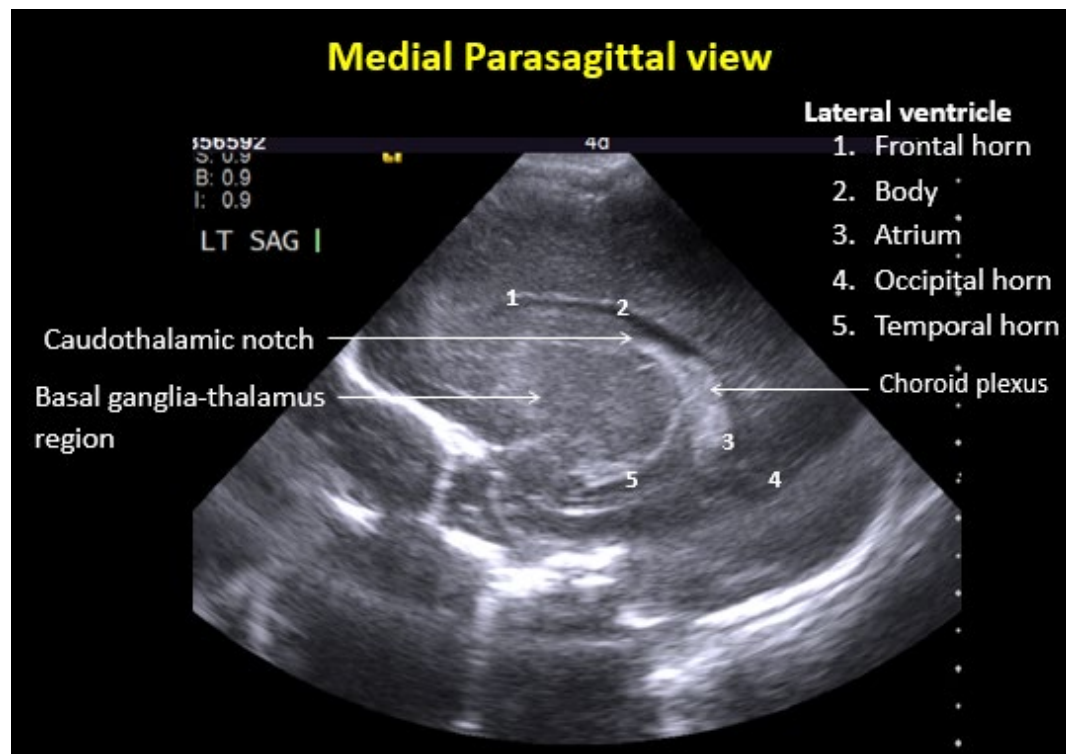


Figure 26: Lateral parasagittal view (Right and left)

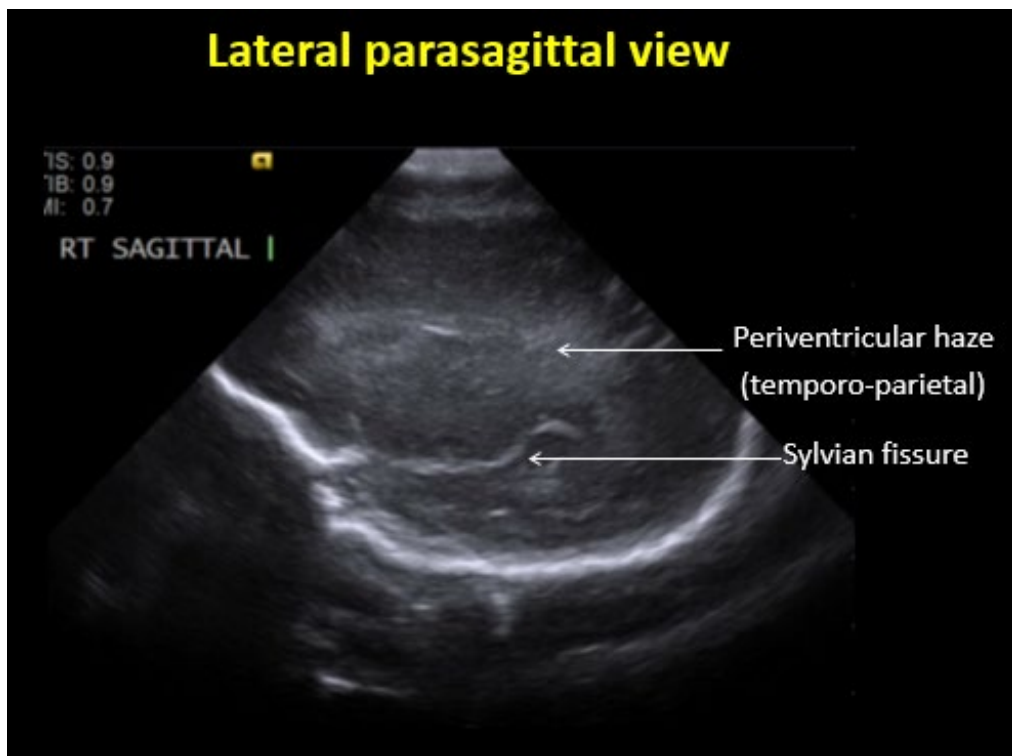


Figure 27: Posterior fontanelle sagittal view

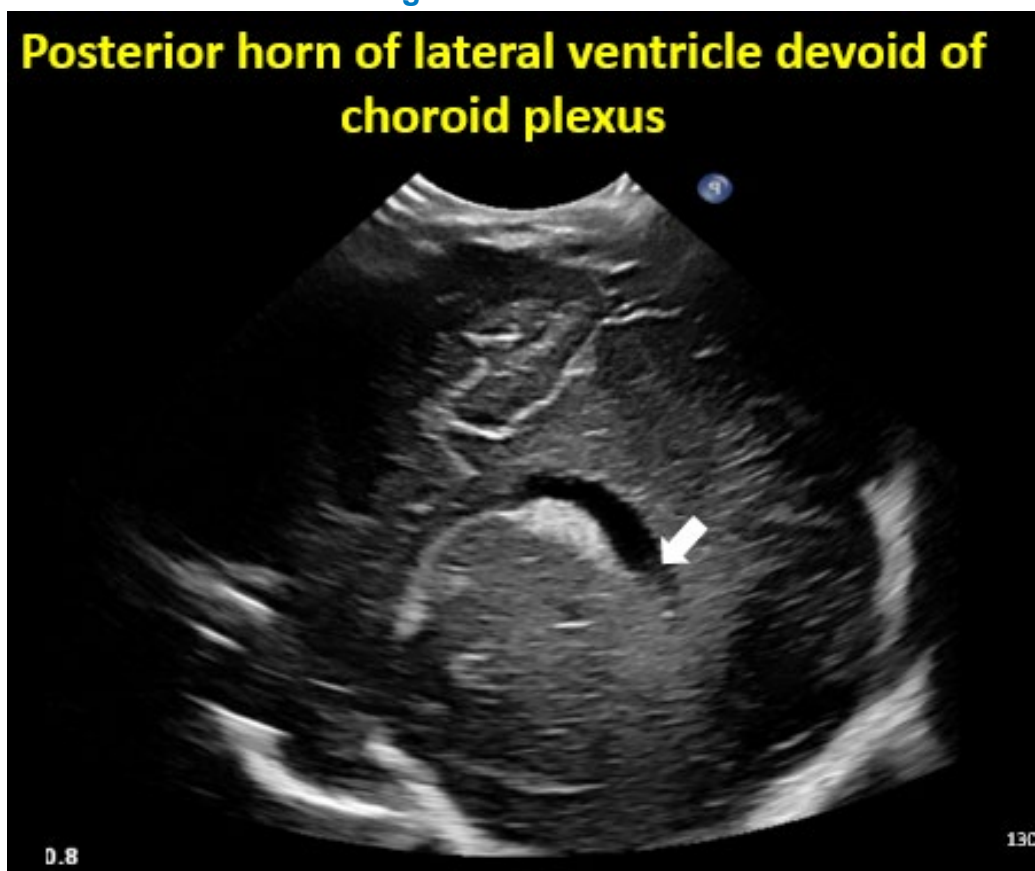




Figure 28: Mastoid view

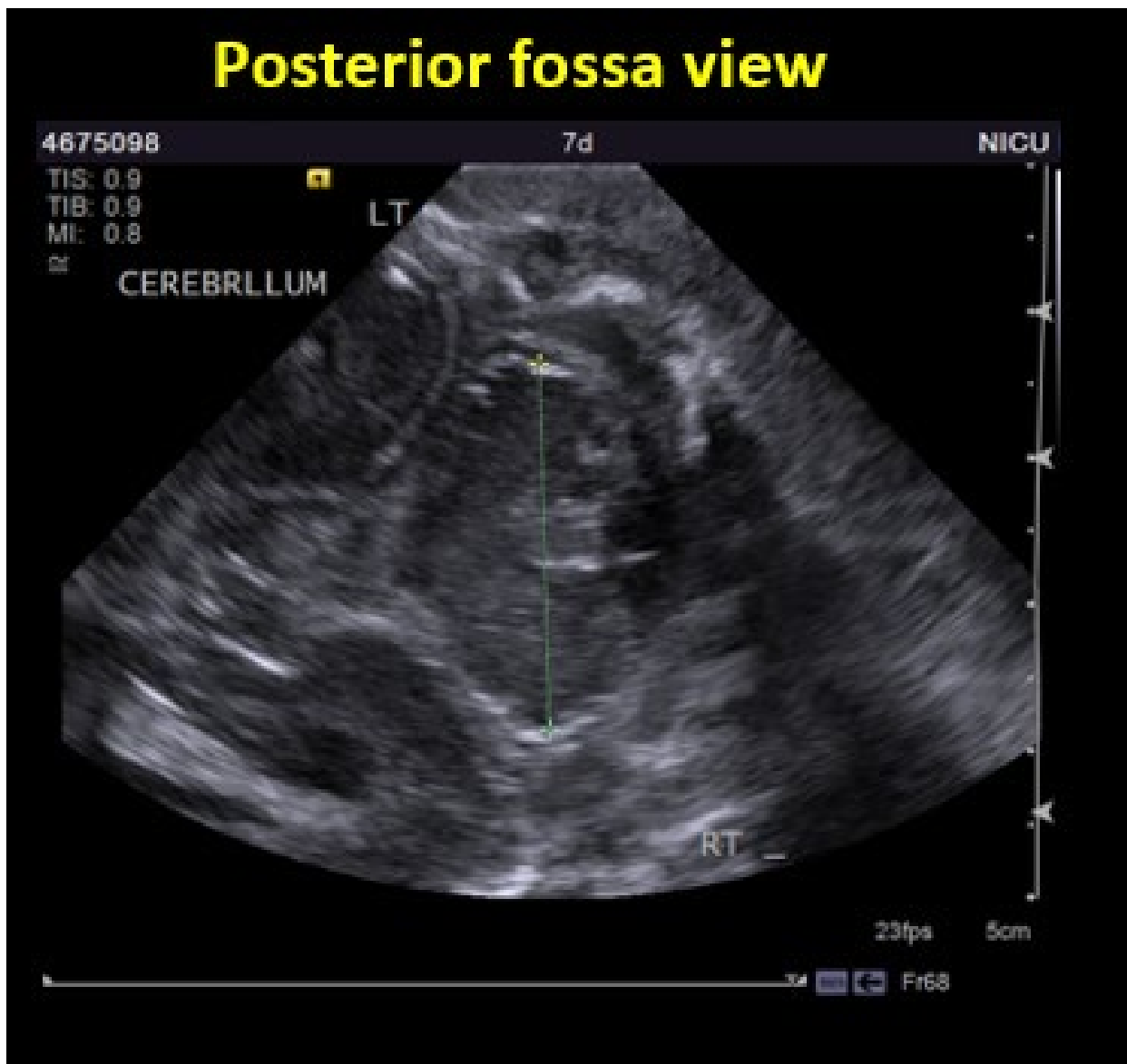
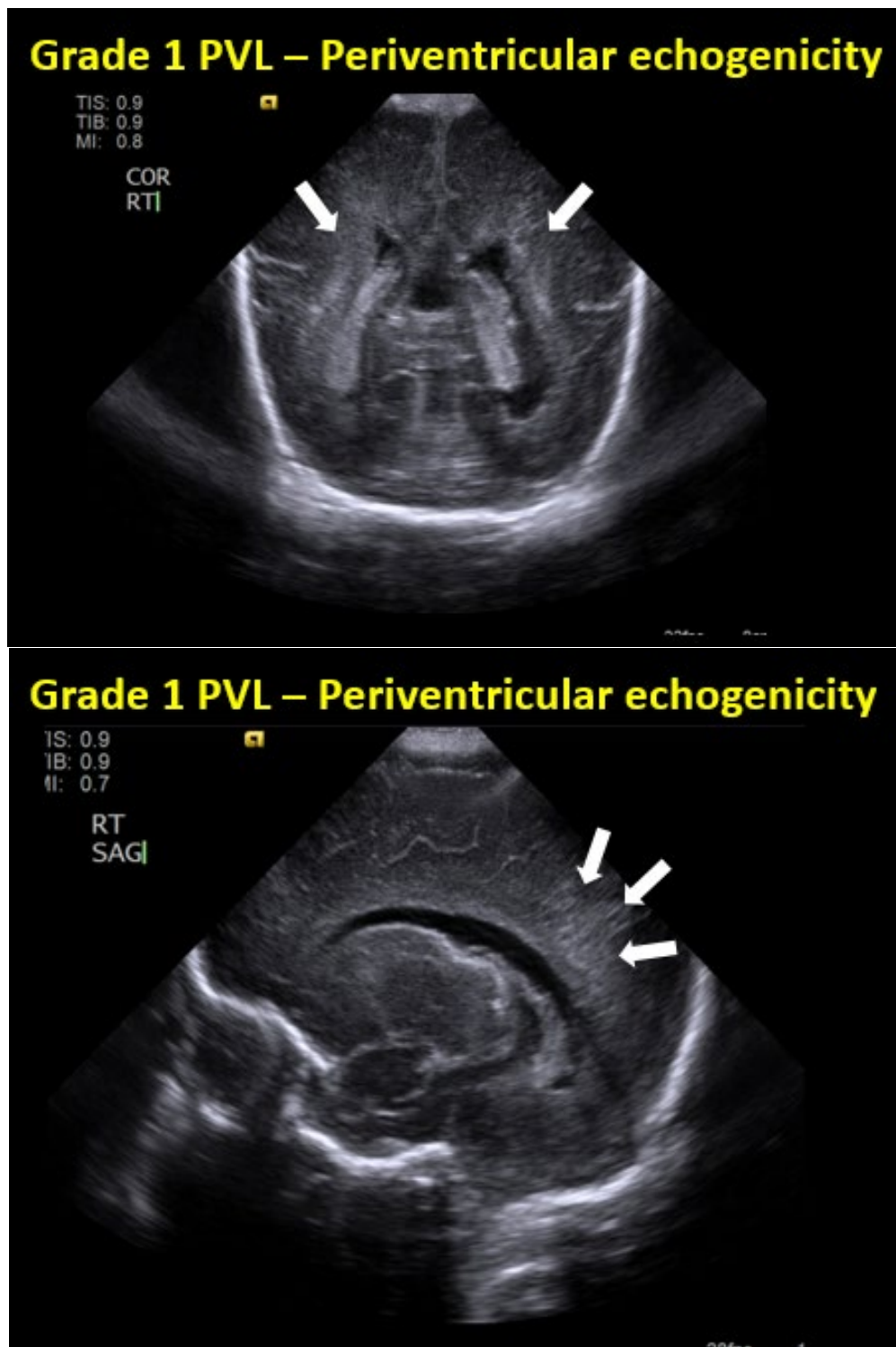
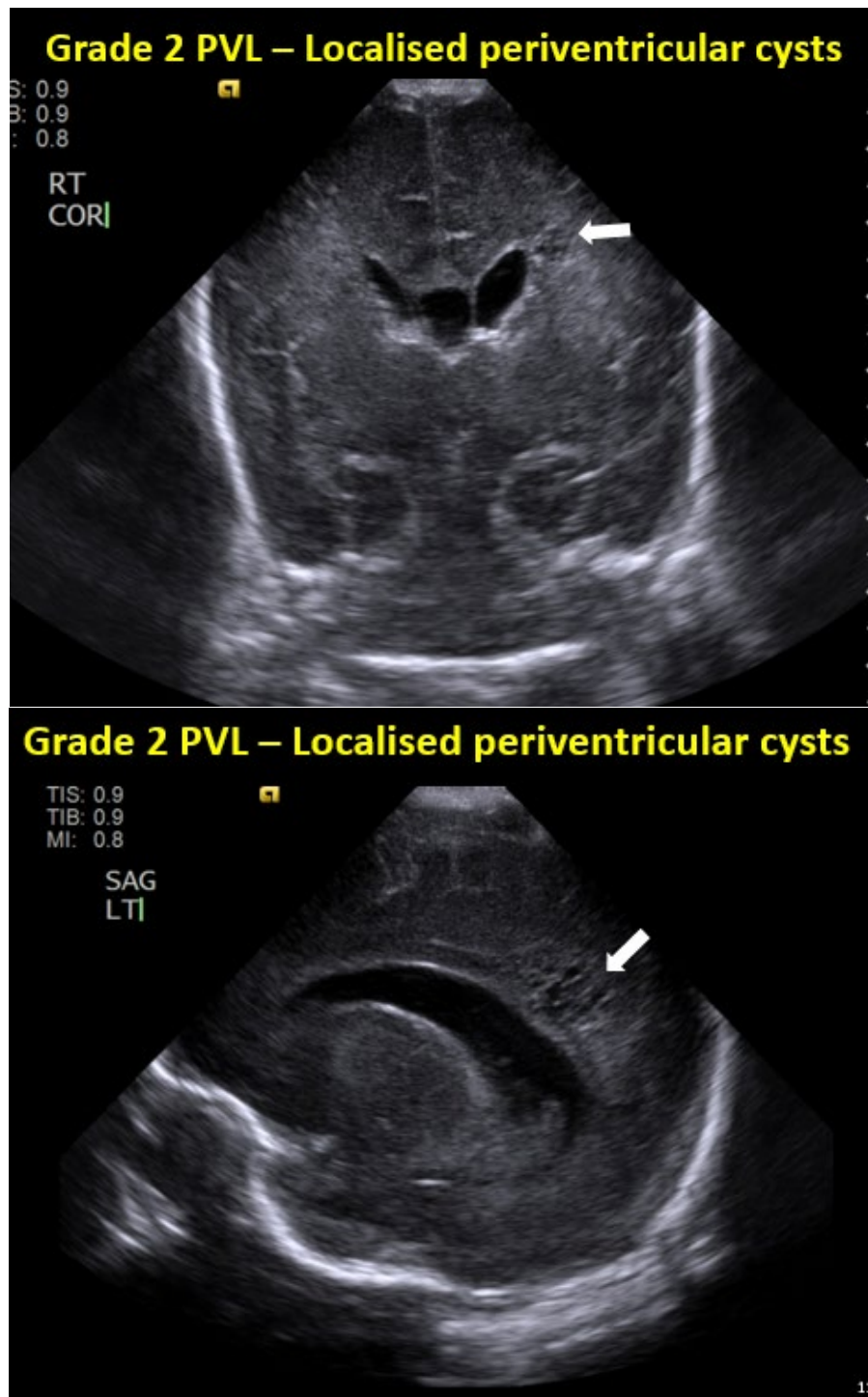


Figure 29: Periventricular echogenicity



**Figure 30: Coronal and sagittal views showing localised periventricular echolucencies suggestive of periventricular leukomalacia**



**Figure 31: Coronal and sagittal views showing more extensive periventricular echolucencies suggestive of periventricular leukomalacia**

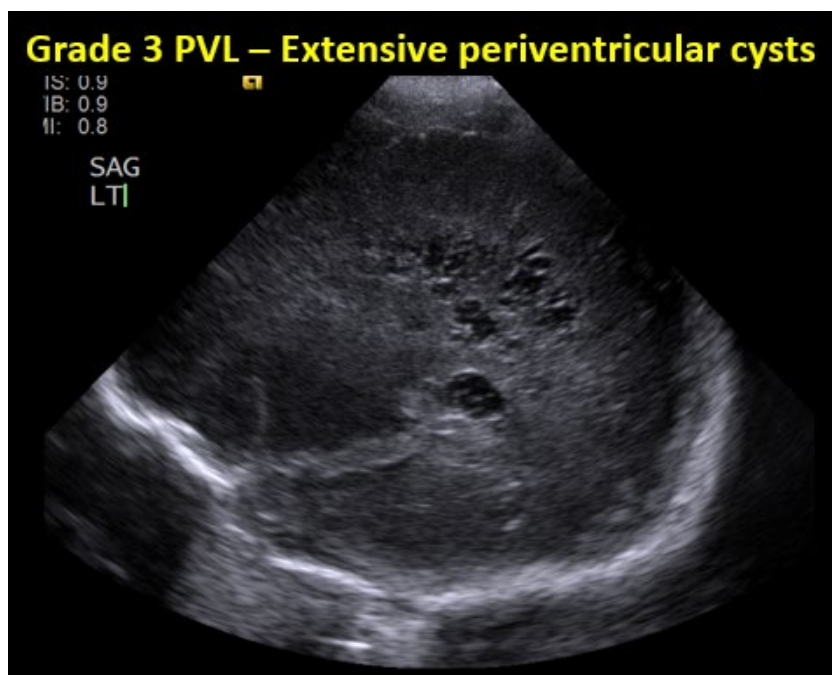
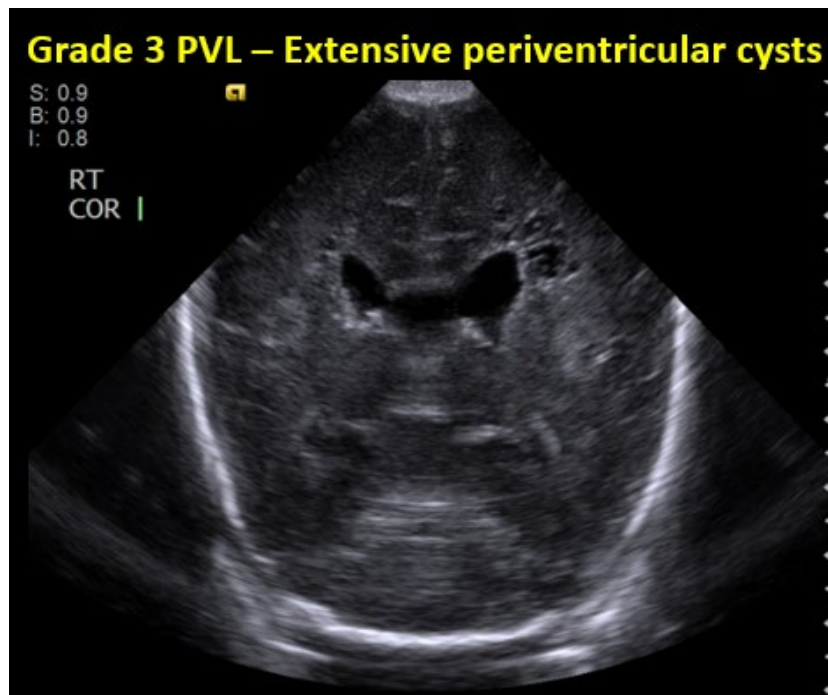


Figure 32: Extensive frontoparietal periventricular leukomalacia

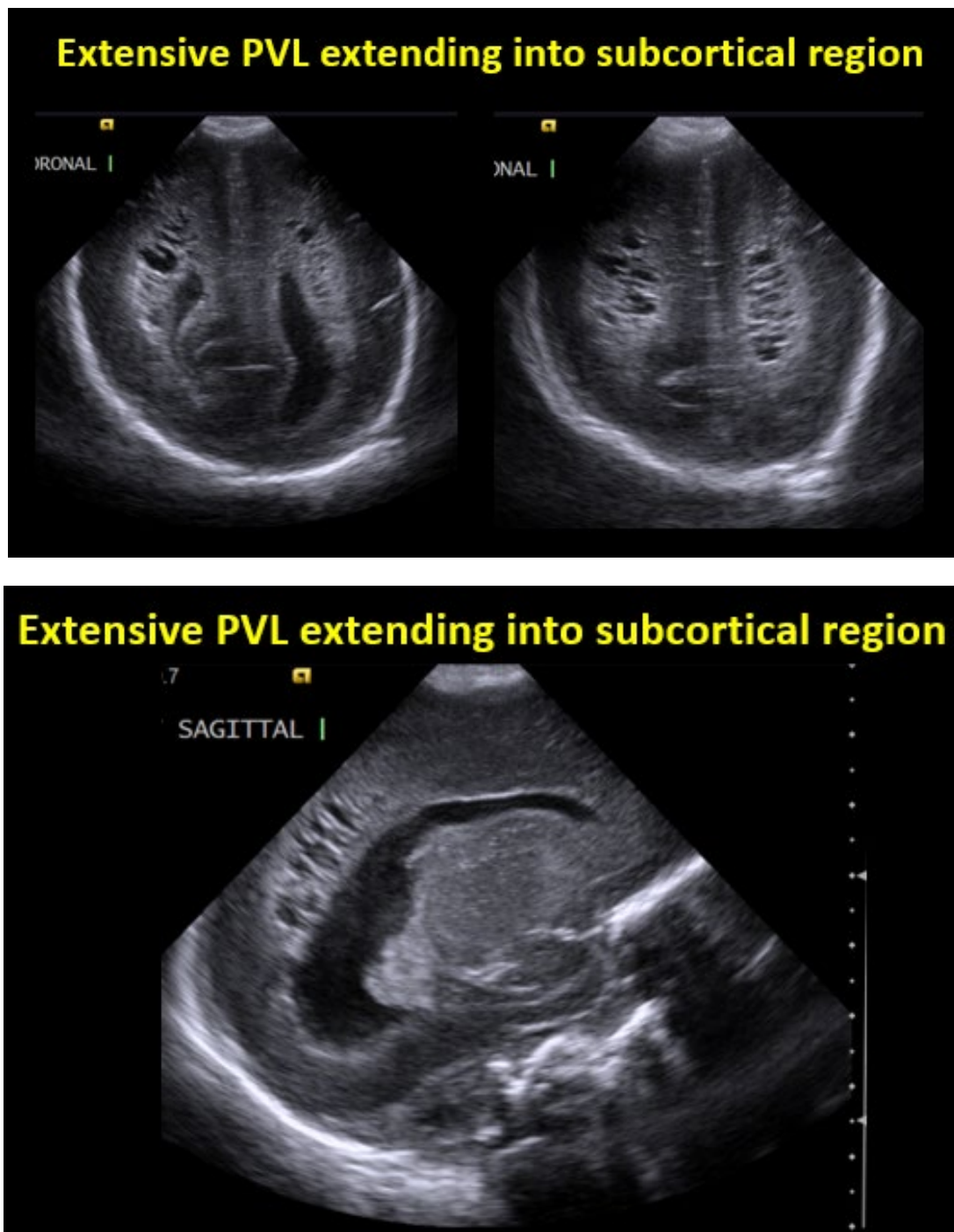




Figure 33: Grade 1 germinal matrix haemorrhage

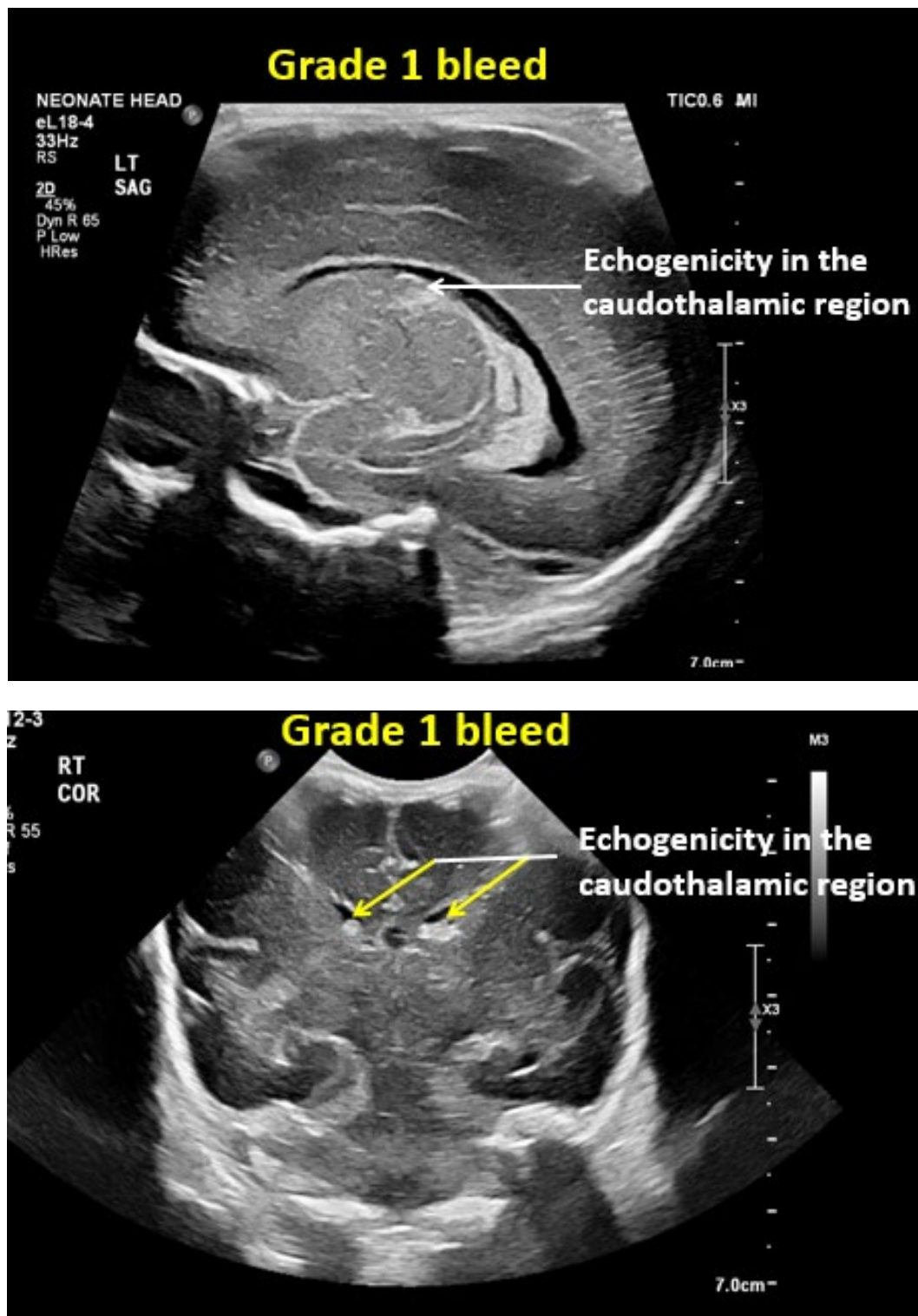


Figure 34: Grade 2 IVH

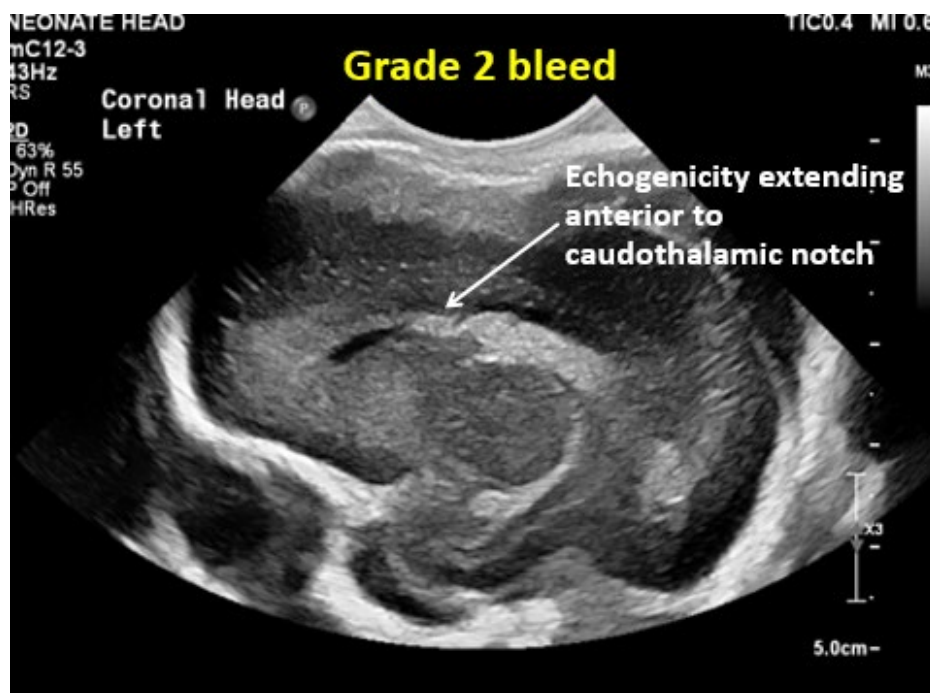
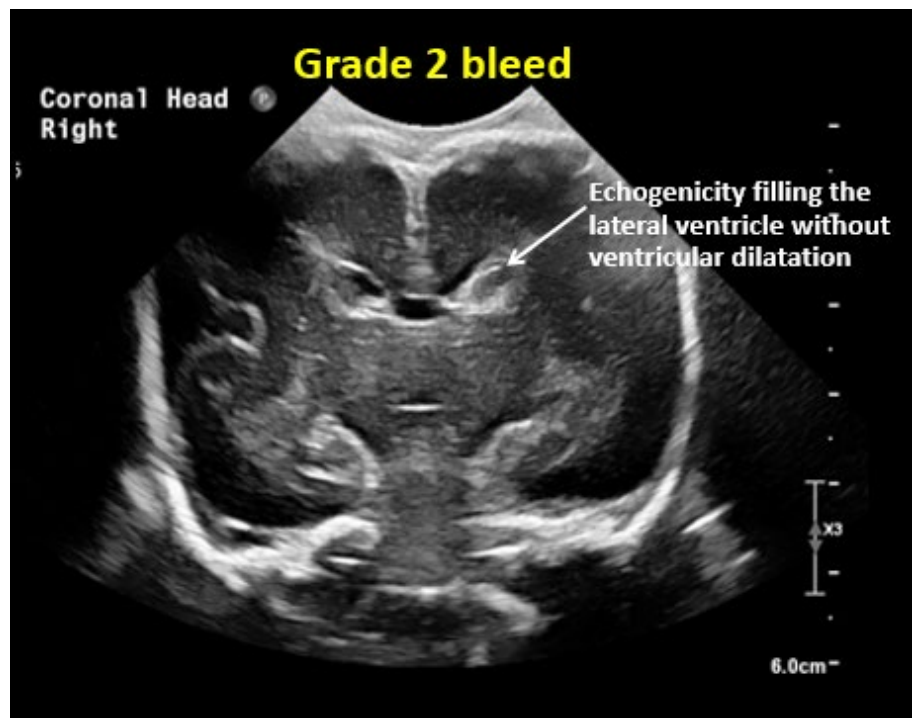


Figure 35: Grade 2 IVH into occipital horn of lateral ventricle

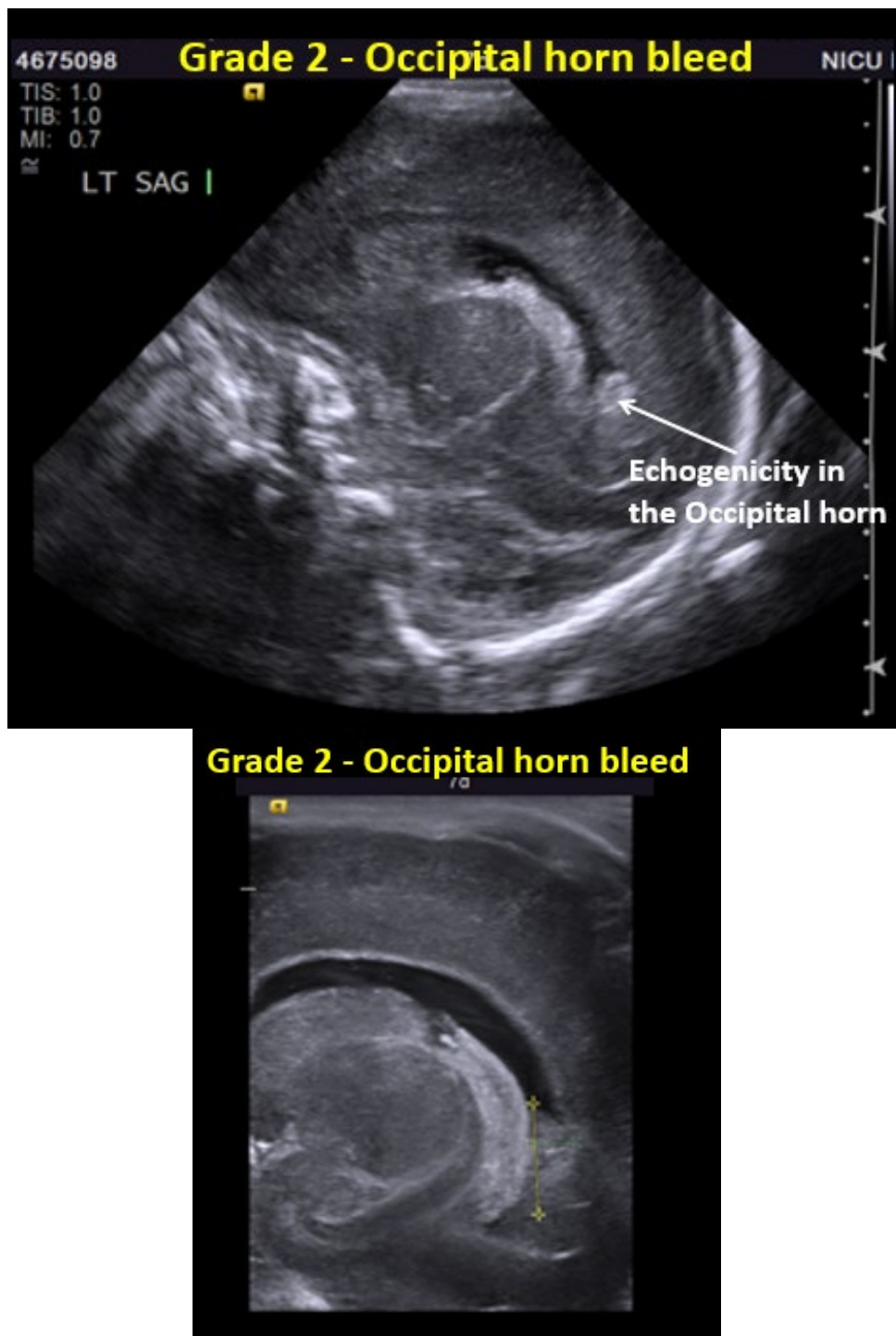




Figure 36: Grade 3 IVH

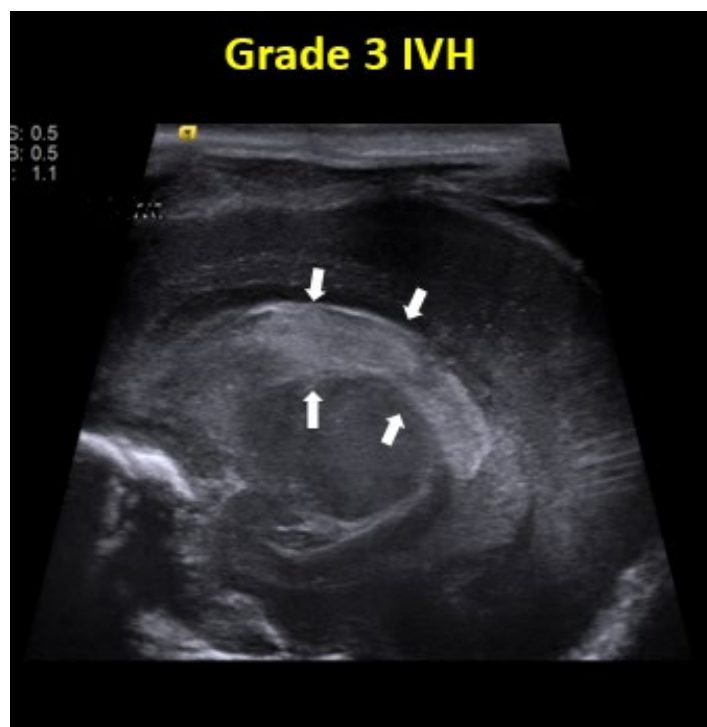
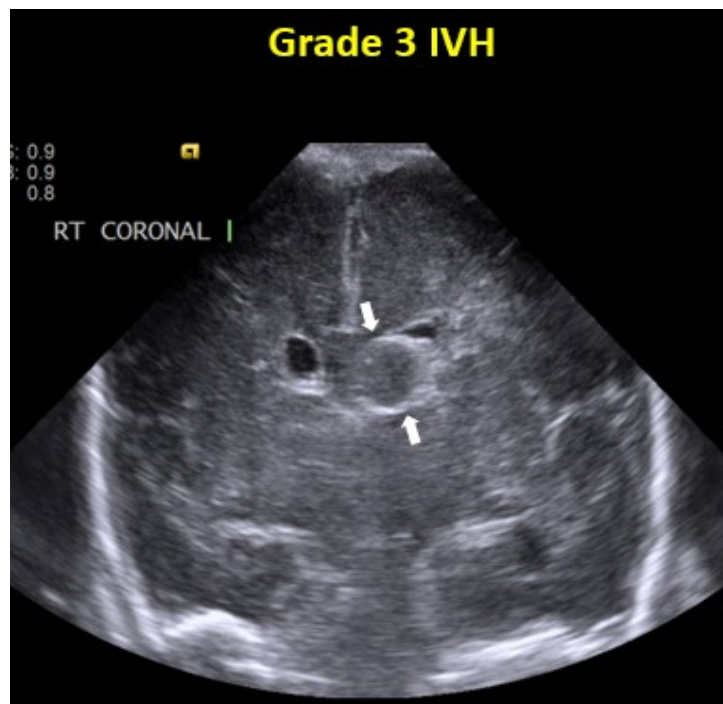
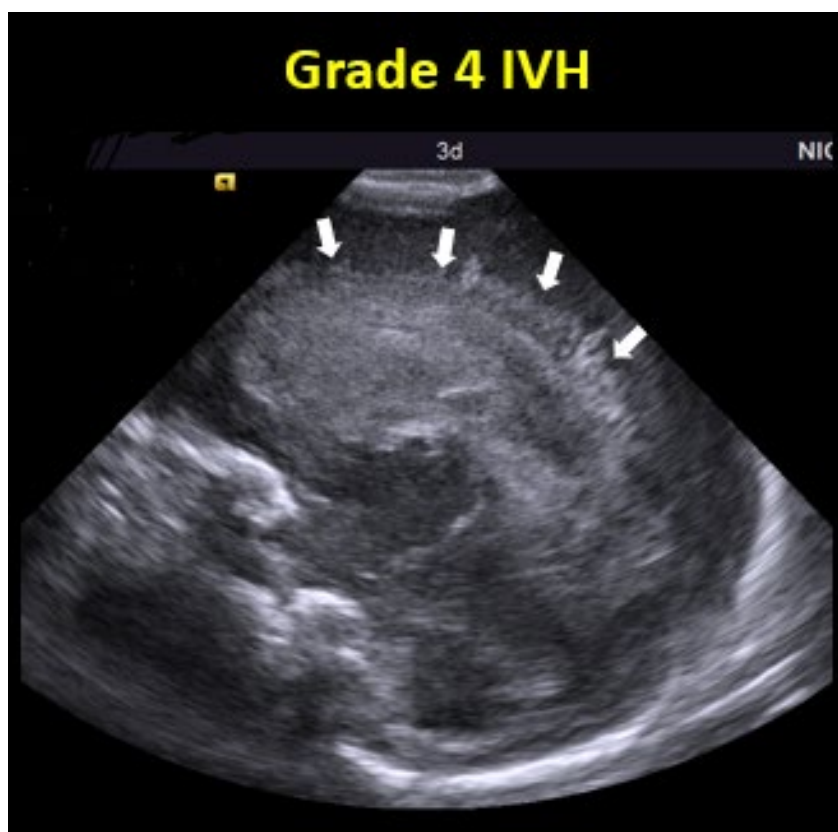
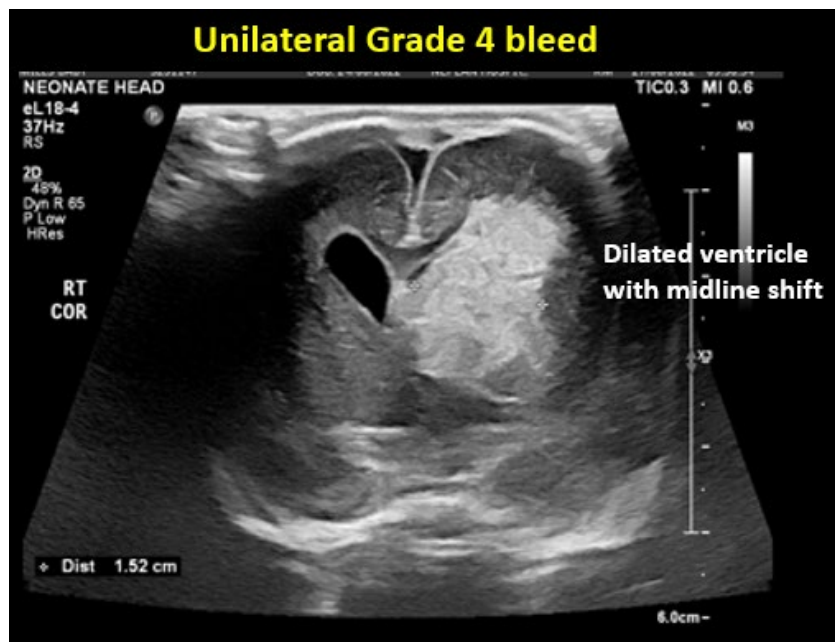


Figure 37: Grade 4 IVH with midline shift



## References

1. Maller VV, Cohen HL. Neonatal Head Ultrasound: A Review and Update—Part 1: Techniques and Evaluation of the Premature Neonate. *Ultrasound quarterly*. 2019;35(3):202-211.
2. Papile L-A, Burstein J, Burstein R, Koffler H. Incidence and evolution of subependymal and intraventricular hemorrhage: a study of infants with birth weights less than 1,500 gm. *The Journal of pediatrics*. 1978;92(4):529-534.
3. Harris D, Teele R, Bloomfield F, Harding J. Does variation in interpretation of ultrasonograms account for the variation in the incidence of germinal matrix/intraventricular haemorrhage between newborn intensive care units in New Zealand? *Archives of Disease in Childhood-Fetal and Neonatal Edition*. 2005;90(6):F494-F499.
4. Carteaux P, Cohen H, Check J, et al. Evaluation and development of potentially better practices for the prevention of brain hemorrhage and ischemic brain injury in very low birth weight infants. *Pediatrics*. 2003;111(Supplement E1):e489-e496.
5. Pekcevik Y, Ozer EA, Guleryuz H. Cranial sonography in extremely preterm infants. *Journal of Clinical Ultrasound*. 2014;42(5):283-290.
6. Dudink J, Steggerda SJ, Horsch S. State-of-the-art neonatal cerebral ultrasound: technique and reporting. *Pediatric Research*. 2020;87(1):3-12.
7. Murphy N, Rennie J, Cooke R. Cranial ultrasound assessment of gestational age in low birthweight infants. *Archives of disease in childhood*. 1989;64(4):569-572.
8. Naidich T, Grant J, Altman N, et al. The developing cerebral surface. Preliminary report on the patterns of sulcal and gyral maturation--anatomy, Ultrasound, and magnetic resonance imaging. *Neuroimaging Clinics of North America*. 1994;4(2):201-240.
9. Leijser LM, de Vries LS, Cowan FM. Using cerebral Ultrasound effectively in the newborn infant. *Early human development*. 2006;82(12):827-835.
10. Enríquez G, Correa F, Lucaya J, Piqueras J, Aso C, Ortega A. Potential pitfalls in cranial sonography. *Pediatric radiology*. 2003;33(2):110-117.
11. Lowe LH, Bailey Z. State-of-the-art cranial sonography: part 2, pitfalls and variants. *American Journal of Roentgenology*. 2011;196(5):1034-1039.
12. Epelman M, Daneman A, Blaser SI, et al. Differential diagnosis of intracranial cystic lesions at head US: correlation with CT and MR imaging. *Radiographics*. 2006;26(1):173-196.
13. Yoon H-K, Cho SW. Neonatal head ultrasound: a systematic approach to congenital Central Nervous System anomalies. A pictorial essay. *Medical ultrasonography*. 2016;18(3):386-393.
14. van Wezel-Meijler G, Steggerda SJ, Leijser LM. Cranial ultrasonography in neonates: role and limitations. Paper presented at: Seminars in perinatology2010.
15. van Wezel-Meijler G, Leijser LM, Wiggers-de Bruïne FT, Steggerda SJ, van der Grond J, Walther FJ. Diffuse hyperechogenicity of basal ganglia and thalami in preterm neonates: a physiologic finding? *Radiology*. 2011;258(3):944-950.
16. Di Salvo DN. A new view of the neonatal brain: clinical utility of supplemental neurologic US imaging windows. *Radiographics*. 2001;21(4):943-955.
17. Anderson NG, Hay R, Hutchings M, Whitehead M, Darlow B. Posterior fontanelle cranial ultrasound: anatomic and sonographic correlation. *Early human development*. 1995;42(2):141-152.
18. Correa F, Enríquez G, Rosselló J, et al. Posterior fontanelle sonography: an acoustic window into the neonatal brain. *American Journal of Neuroradiology*. 2004;25(7):1274-1282.
19. Buckley K, Taylor G, Estroff J, Barnewolt C, Share J, Paltiel H. Use of the mastoid fontanelle for improved sonographic visualisation of the neonatal midbrain and posterior fossa. *AJR American journal of roentgenology*. 1997;168(4):1021-1025.
20. Steggerda S, van Wezel-Meijler G. Cranial ultrasonography of the immature cerebellum: role and limitations. Paper presented at: Seminars in Fetal and Neonatal Medicine2016.
21. de Vries LS, Eken P, Dubowitz LM. The spectrum of leukomalacia using cranial Ultrasound. *Behavioural brain research*. 1992;49(1):1-6.